Virginia Commonwealth University

VCU Scholars Compass

Theses and Dissertations

Graduate School

2015

Interplay between Artemis and TDP1 in sensitivity to radiomimetic agents

Ajinkya S. Kawale
Virginia Commonwealth University

INTERPLAY BETWEEN ARTEMIS AND TDP1 IN SENSITIVITY TO RADIOMIMETIC

AGENTS

A thesis submitted in partial fulfillment of the requirements for the degree of Master of

Science at Virginia Commonwealth University

By

Ajinkya Kawale

B.Tech in Biotechnology, Dr. D.Y.Patil University, India, 2013

Advisor: Dr. Lawrence F. Povirk, Professor, Department of Pharmacology and Toxicology

Virginia Commonwealth University

Richmond, Virginia,

April, 2015

ACKNOWLEDGEMENT

TABLE OF CONTENTS

LIST OF FIGURES

viii

LIST OF TABLES

LIST OF ABBREVIATIONS

′	Prime
°C	degrees Centigrade
μ	Mu
μm	micrometer
53BP1	p53 binding protein
A	Adenine
AP	Apurinic/ Apyrimidinic
APE1	Apurinic/ Apyrimidinic Endonuclease 1
A-T	Ataxia Telangiectasia
ATM	Ataxia Telangiectasia Mutated
ATP	Adenosine Triphosphate
BIA	Biochemical Induction Assay
BRCT	Breast Cancer Susceptibility Gene C Terminus
BSA	Bovine Serum Albumin
C	Cytosine
cm	centimetre

CO_2	Carbon dioxide
Cy5	Cyanine 5
DAPI	4'-6-diamidino-2-phenylindole
DCLRE1C	DNA Cross-Link Repair 1C
DMSO	Dimethyl Sulfoxide
DNA	Deoxyribose Nucleic Acid
DNA-PKcs	DNA Protein Kinase catalytic subunit
dRP	deoxyribosephosphate
DSBs	Double-strand Breaks
DTT	Dithiothrietol
EDTA	ethylene diamine tetraacetic acid
FBS	Fetal Bovine Serum
G	Guanine
G1	Growth 1
G2	Growth 2
Gy	Gray
H	Histidine
HAc	Acetic Acid
HEPES	4-(2-hydroxyethyl)-1-piperazineethanesulfonic acid
HKN	Histidine Lysine Asparagine
HR	Homologous Recombination

IR	Ionising radiation
K	Potassium
KCl	Potassium Chloride
KDa	KiloDalton
M	Mitosis
M	Molar
Mg	Magnesium
Min	minutes
mL	millilitre
N_2	Nitrogen
NaCl	Sodium Chloride
NaVO4	Sodium Orthovanadate
NCS	Neocarzinostatin
NCS-Chrom	Neocarzinostatin – chromophore
NHEJ	Non-Homologous End Joining
NP-40	nonyl phenoxypolyethoxylethanol
Pac	Puromycin N-Acetyl transferase
PBS	phosphate buffered saline
PCR	Polymerase Chain Reaction
PE	plating efficiency
PI	Propidium iodide

PLD	Phospholipase D
pM	picomolar
PMSF	phenylmethanesulfonyl fluoride
PMT	photomultiplier tube
PNKP	Polynucleotide Kinase Phosphatase
R	Arginine
ROS	Reactive Oxygen Species
RPM	rotations per minute
RPMI	Roosevelt Park Memorial Institute
RS-SCID	Radiosensitivie – Severe combined Immunodeficiency
S. cerevisiae	Saccharomyces cerevisiae
SCAN1	Spinocerebellar Ataxia with Axonal Neuropathy
SEM	Standard Error of Mean
SF	surviving fraction
shRNA	short hairpin ribonucleic acid
S-phase	Synthesis phase
SSBs	Single-strand Breaks
T	Thymine
TBE	Tris Borate EDTA
TDP1	Tyrosyl-DNA Phosphodiesterase 1
TEMED	N', N', N', N'-tetramethylethylene diamine

Top I	Topoisomerase I
TX	Texas
UV	Ultraviolet
V(D)J	Variable (Discrete) Joining
W	Watts
XLF	XRCC4-like factor
XRCC4	X-Ray Cross Complementing Protein 4
Y	tyrosine
β	Beta
γ	Gamma
λ	Lambda

ABSTRACT

INTERPLAY BETWEEN ARTEMIS AND TDP1 IN SENSITIVITY TO RADIOMIMETIC

AGENTS

Ajinkya Kawale, B.Tech

A thesis submitted in partial fulfillment of the requirements for the degree of Master of Science

at Virginia Commonwealth University

Virginia Commonwealth University, 2015

Advisor: Dr. Lawrence F. Povirk, Professor, Department of Pharmacology and Toxicology

DNA double-strand breaks containing unligatable termini are potent cytotoxic lesions leading to

cell death or growth arrest. Artemis, which is associated with the Non-Homologous End Joining

(NHEJ) pathway, is the major end processing nuclease that resolves unligatable termini, especially the 3′ blocks, by nucleolytic trimming. Tyrosyl-DNA Phosphodiesterase 1 (TDP1) is an enzyme which is biochemically competent in 3′-phosphoglycolate processing. The purpose of this study is to investigate if TDP1 is an end-processing enzyme involved in the NHEJ pathway. Clonogenic Survival assays using shRNA-mediated TDP1 knockdown and Artemis knockout (Artemis-/-) in HCT116 cells showed increased sensitivity to Neocarzinostatin (NCS) and Calicheamicin, radiomimetic drugs that produce 3′-phosphoglycolate-terminated double-strand breaks. Thus, a cell line with combined deficiency in Artemis and TDP1 was generated by infecting Artemis-/- single mutants with a lentivirus expressing a TDP1 shRNA. Positive clones were screened for maximum TDP1 knockdown which was found to be 10X. Clonogenic survival assays carried out on shTDP1 & Artemis-/- single mutants and the Artemis-/-.shTDP1 double mutants showed similar sensitivity to Calicheamicin and NCS. Immunofluorescence studies on Art-/- and Art-/-.shTDP1 mutants also showed a similar increase in persistent 53BP1 foci, a measure of DNA damage, after treatment with NCS. Cell cycle analysis studies showed all these mutants arrest in G1 phase of the cell cycle after treatment with NCS. Thus, taken all together, surprisingly, these experiments suggest that TDP1 functions are epistatic with Artemis in the NHEJ pathway for repair of Calicheamicin- and NCS-mediated DNA damage.

1. INTRODUCTION

The genome of an organism is under constant threat from various sources that may result in genomic instability. These endogenous as well as exogenous sources of cellular damage are extremely harmful and undermine the genomic integrity resulting in massive amounts of DNA lesions of various types every day in every organism. Endogenous DNA damage may come from intracellular production of reactive oxygen species (ROS); from normal metabolic byproducts; especially from the process of oxidative deamination, also from V(D)J recombination as well as some replication errors. There are five main types of DNA lesions due to endogenous cellular processes: oxidation of bases (e.g. 8-oxoG), alkylation of bases (e.g. methylation), hydrolysis of bases (e g. deamination, depurination), bulky adduct formation and mismatch of bases (due to errors in DNA replication) (De Bont & van Larebeke, 2004). Exogenous DNA damage may result from: exposure to ultraviolet light B (UV-B light causes crosslinking creating pyrimidine dimers, called direct DNA damage; UV-A light creates mostly free radicals), thermal disruption (causes increased rate of depurination and single-strand breaks), industrial chemicals (e.g. hydrogen peroxide, polycyclic aromatic hydrocarbons), or exposure of ionizing radiation (causes bases oxidation, single-strand breaks and double-strand breaks) (Langer et al., 1975). Base damage and SSBs can subsequently

lead to DSBs when encountered by DNA replication or transcriptional machinery (Branzei & Foiani, 2007; Mahajan et al., 2002). Two-hundred million gamma rays pass through each of us every hour due to the natural decay of the radionuclides occurring in the earth (Lieber at al. 2003). Of all the different types of lesions encountered by a cell, the most potent cytotoxic lesions are DNA Double-Strand Breaks (DSBs). DSBs are formed due to a variety of endogenous sources including immunological process such as V(D)J recombination (a process which involved genetic rearrangements for the maturation of B- and T-lymphocytes), imperfect topoisomerase reactions and oxidative stress along with a few exogenous sources like ionizing radiation and radiomimetic drugs (Povirk, 2013). If left unrepaired, these DSBs may result in chromosomal aberrations leading to tumorigenesis or cell death. Thus, in order to survive this constant assault on their genome and to preserve the genomic integrity in the progeny, cells have evolved two DSB repair pathways which are quite different from each other, Non-Homologous End Joining (NHEJ) and Homologous Recombination (HR).

NHEJ is the principal pathway for repair of these DSBs and mediates direct re-ligation of the damaged DNA strands after end-processing. Thus, unlike HR, it does not require a homologous template for its repair and hence is not restricted to a particular phase of the cell cycle. It is active throughout the cell cycle unlike HR, which is active only in the late S and G2 phase. In fact, NHEJ is the only DSB repair pathway active in G1 phase when HR is absent. As NHEJ does not require a template for repair, it may induce a few errors during the repair process often characterized by the loss of a few nucleotides whereas HR is typically an error free repair mechanism. The most interesting aspect of NHEJ is its ability to accept a diversity of substrates and convert them to joined products. This demands a great flexibility in mechanical interaction of involved proteins to accept a plethora of different substrates that are generally produced following exposure to free

radicals. Reactive oxygen species can interact with DNA to produce multiply damaged sites with different lengths of overhangs, end termini blocked with oxidation products and several types of base damage, most commonly 8-oxoguanine and thymine glycols. These variously modified overhangs are joined by NHEJ regardless of the sequence, overhang length or DNA end products.

1.1 Non-Homologous End Joining (NHEJ):

The process of NHEJ could be divided into 4 general steps: 1) The broken ends of the DNA molecule are captured, 2) the two broken DNA ends brought together through the formation of a molecular bridge, 3) Processing of the broken DNA ends and 4) subsequent ligation of the DNA ends followed by the disassembly of the NHEJ complex. Although, the process looks deceitfully simple, in actuality, it is an incredibly intricate, orchestrated process involving a variety of proteins performing highly specific functions in order to achieve the aim of repairing deleterious DSBs.

The process of NHEJ begins with the recruitment of Ku at the double-strand break site (Mari et al. 2006, Davis & Chen 2013, Lieber et al. 2003)*.* Ku is a heterodimer comprising of two subunits, Ku70 and Ku80. Ku is highly abundant in cells with 4-5 X 10^5 molecules of Ku per cell and it has an extraordinarily high affinity for DNA ends with equilibrium constant of around 5 X 10^{-10} M allowing it to immediately localize to DSBs. (Lieber et al. 2003) X-Ray Crystallography studies have revealed that the structure of Ku is ring-shaped which fits the DNA perfectly inside it, allowing it to slide onto the DNA strands. Studies have also revealed that Ku binds to the Phosphodiester backbone of the DNA instead of the bases, indicating that the binding is not sequence-specific. Recruitment of Ku also has been linked with aligning of the DNA strands, maintaining their stability and protecting them from non-specific degradation. Once Ku has been recruited to the DSB site, the DNA-Ku complex acts as a scaffold to recruit the DNA Protein

Kinase catalytic subunit (DNA-PKcs) at the break site. Atomic force Microscopy studies show that DNA-PKcs molecules on each end of a DSB form a bridge between the two ends (Lieber et al. 2003) ultimately leading to the formation of a synaptic complex involving DNA ends, Ku and DNA-PKcs. The presence of unphosphorylated DNA-PKcs prevents the end-processing and ligation of DNA ends thereby protecting them from premature degradation. Auto-phosphorylation of DNA-PKcs results in the DNA ends being accessible to the end-processing enzymes and ligases. Different types of DSB lesions are generated in response to ionizing radiation. The majority of these lesions are unligatable and as such have to be processed before the ends can be ligated together. Many enzymes have been implicated to perform these roles of resection of DNA ends and removal of 3′- and 5′- blocks in order to make the ends ligatable. Artemis nuclease is the most studied end-processing enzyme involved in resection of single-strand overhangs. Artemis has intrinsic 5′ exonuclease activity in the absence of DNA-PKcs (Bunting & Nussenzweig, 2013). Artemis is phosphorylated by DNA-PKcs and Artemis-DNA-PKcs complex can act as an endonuclease at 3′ and 5′ overhangs (Lieber et al. 2003). A large number of end-processing enzymes have been shown to remove 3′- and 5′- blocks from the DNA ends. Some of these blocks and the enzymes involved in processing of those blocks include 3′-phosphates and 5′-hydroxyls which are processed by Polynucleotide Kinase Phosphatase (PNKP), 3′-phosphoglycolates removed by TDP1, APE1 and Artemis (Bunting & Nussenzweig, 2013).

The final stage in the repair of DSBs through the NHEJ pathway involves gap filling followed by ligation of the DNA ends that have been aligned, tethered and processed by making them ligatable. DNA polymerases μ and λ can bind to the KU-DNA-PK complexes by their BRCT domains located in the N-terminal portion of the polymerases carrying out DNA strand synthesis (Weterings & Chen, 2008). The enzyme involved in the ligation of these ends is DNA Ligase IV, the principal

ligase required for NHEJ. It forms a complex with two proteins, X-ray Cross Complementing

Protein 4 (XRCC4) and XRCC4-like factor (XLF) and its activity is enhanced in the presence of

XRCC4 and XLF (Lees-Miller, S., & Meek, K. 2003).
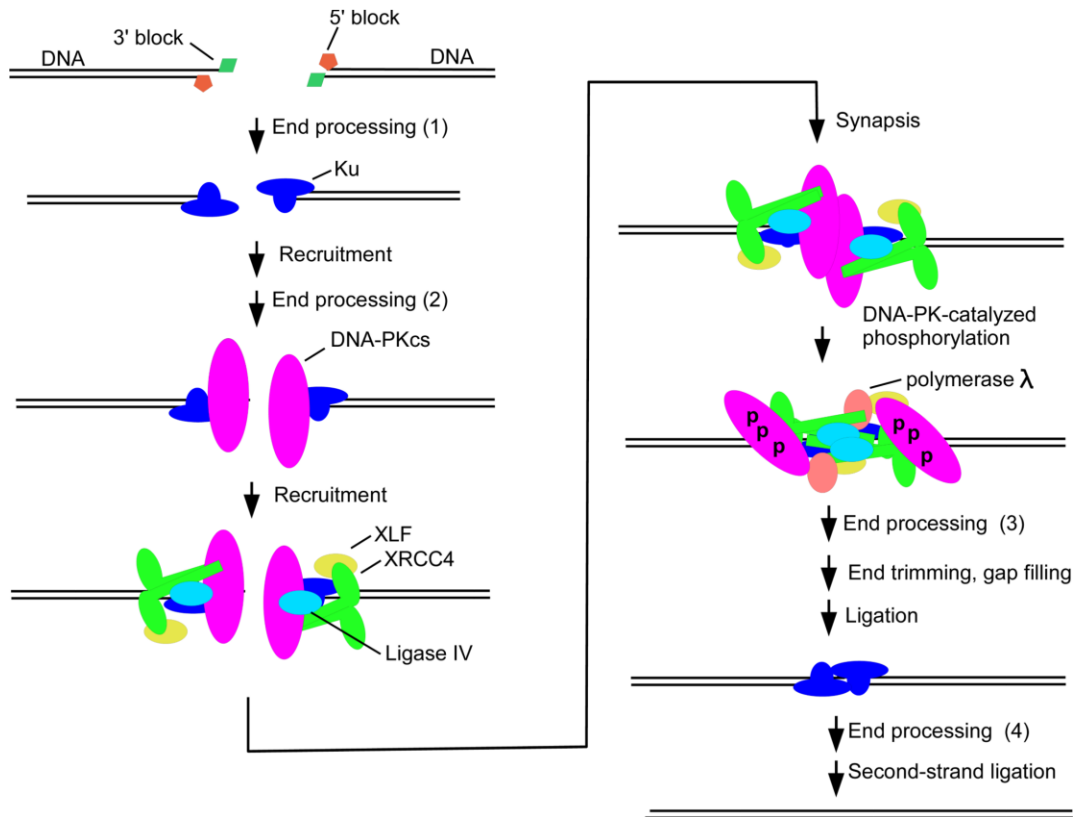
Figure 1- Non-Homologous End Joining (NHEJ)

Ku binds to DNA ends and recruits DNA-PKcs, the XRCC4 / DNA ligase IV complex, and

XLF. Synapsis of two DSB ends triggers DNA-PKcs autophosphorylation. The ends formed

following DNA damage are unligatable which are here referred to as 5′- and 3′-terminal blocks.

DNA-PKcs autophosphorylation-mediated resolution of these blocks by various end-processing

enzymes leads to the production of ligatable ends allowing gap filling by polymerase λ, and

finally ligation by DNA ligase IV. Numbers 1-4 show various stages at which end-processing

could occur. (Povirk, L.F. 2012)

1.2 Tyrosyl-DNA Phosphodiesterase 1 (TDP1):

During DNA replication, the movement of the replication fork resulting in local unwinding of the DNA causes supercoiling ahead of the replication fork. Topoisomerase I helps relax these supercoils in the DNA by transiently cleaving one of the DNA strands via a nucleophilic attack by its Tyrosine-723 amino acid residue on the phosphodiester backbone, unwinding it through the other strand. A second transesterification reaction leads to the religation of the DNA strands to release Topoisomerase I (Pommier, Y. et al 2014). In a few rare cases, however, Topoisomerase I becomes covalently attached to the DNA leading to the formation of irreversible TopI-DNA cleavage complexes which are highly cytotoxic. In 1998, Yang and his colleagues discovered an enzyme from the crude extracts of budding yeast *S. cerevisiae* which specifically cleaved the chemical bond that joined the active site tyrosine of Topoisomerase I to the 3′ end of DNA (Yang et.al 1998). Tyrosyl-DNA phosphodiesterase 1 (TDP1) is an enzyme which removes the peptide fragments linked through tyrosine to the 3′ end of DNA in these Topoisomerase I-mediated breaks (Das et al., 2009).

Structure:

TDP1 is a 68 KDa protein with 608 amino acid residues consisting of two domains. Mutational analysis of the active site residues of human TDP1 show that TDP1 is a member of the phospholipase D superfamily and reveal some important structural features of the protein (Interthal et al. 2001). The N-terminal region of the molecule is very poorly conserved among species and is unimportant for the activity of TDP1 in-vitro (Interthal et al. 2001). Deletion of the first 108 amino acid residues did not affect the catalytic activity of TDP1 (Davies at al. 2002). However, in-vivo it may play a role in TDP1 stability and its recruitment. TDP1 differs slightly from other

members of the PLD family as it contains two catalytic HKN motifs ($H_{263}K_{265}N_{283}$ and $H_{493}K_{495}N_{516}$) in contrast to the others that harbor the characteristic HKD motifs. (Pommier, Y. et al 2014).

These two HKN segments interact together to form a single functional active site which is narrow and positively charged in order to accommodate the negatively charged DNA backbone.

Although TDP1 does not require the presence of a cofactor, the catalytic mechanism of TDP1 which is two-step process involves a complex chemical interplay. The initial step involves a nucleophilic attack by the imidazole N_2 atom of the active site Histidine (H263) residue on the DNA-Top1 phosphotyrosyl bond. The other active site Histidine (H493) residue acts as a general acid to donate a proton to the leaving Tyrosyl moiety. This covalent intermediate phosphoamide bond formed between H263 and the 3′-phosphate of the DNA is the characteristic phosphohistidine intermediate formed by the members of the PLD superfamily. In the second step, the other active site Histidine (H493) residue acts as a general base and makes a nucleophilic attack on a neighbouring water molecule thereby activating it. This activated water molecule subsequently hydrolyses the phosphohistidine intermediate and thus releases the DNA molecule from the enzyme. This mechanism leaves a 3′-phosphate group on the DNA which is further acted upon by Polynucleotide Kinase Phosphatase (PNKP) to generate a 3′-hydroxyl group (Pommier, Y. et al 2014). A homozygous mutation in TDP1 (A1478G) which results in the substitution of the H493 residue with an Arginine residue has been linked to a rare, autosomal recessive genetic disorder, Spinocerebellar Ataxia with Axonal Neuropathy (SCAN1). This substitution of the Histidine to an Arginine is thought to disrupt the active site of the enzyme, thus preventing the dissociation of the phosphohistidine intermediate and thereby failing to ligate the single-strand break generated in the DNA. (Takashima, H. et al 2002)
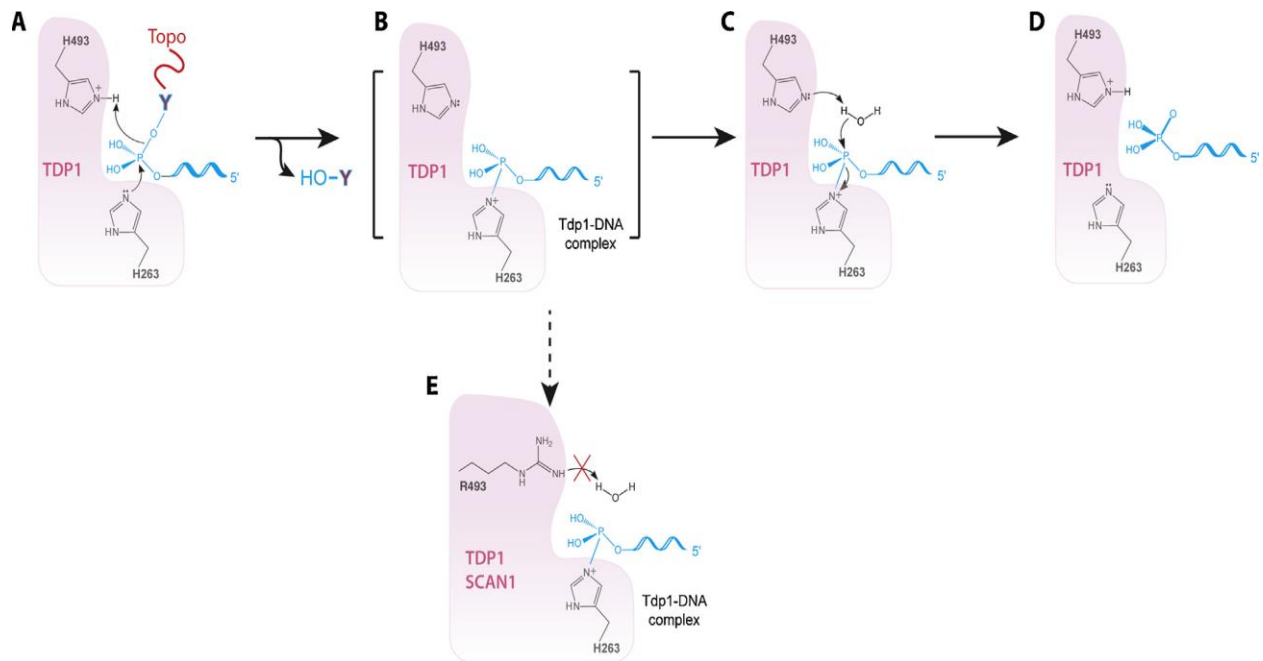
Figure 2 - TDP1 catalytic activity

    A. Nitrogen on H263 makes a nucleophilic attack on the 3′-phosphate of the DNA linked to
Topo I. **B.** This leads to the formation of a TDP1-DNA complex. **C**. H493 of TDP1
makes a nucleophilic attack on a water molecule in the active site of TDP1 which leads to
D. the release of the DNA molecule with a 3′-phosphate from TDP1. **E**. In patients with
SCAN1, H493 is mutated to R493 which cannot make the nucleophilic attack on the
water molecule thus leading to unresolved TDP1-DNA complexes. (Pommier, Y. et al
2014)

Function

TDP1 was first identified as an enzyme in yeast cell extracts involved in the in-vitro hydrolysis of the 3′-phosphotyrosyl moiety containing substrate. The fact that TDP1 can resolve the tyrosine peptide fragments from the 3′-end of DNA in Top1 cleavage complexes is well documented. Although TDP1 cannot remove native Top1 linked to the DNA, it can hydrolyze peptides formed due to degradation or denaturation of Top1 (Pommier et al 2014). Around 50% of the breaks generated by ionising radiation contain 3′-phosphoglycolates at the ends. 3′-Phosphoglycolates are also formed in response to free radical mediated DNA breaks (Zhou et al. 2009) and are present at the double-strand break ends generated by the action of radiomimetic drugs like Calicheamicin, Neocarzinostatin (NCS) and bleomycin (Chaudhry et al. 1999). Whole-cell extracts containing TDP1 were shown to catalyze the conversion of 3′-PG moieties to 3′-phosphates on both single-strand breaks as well as 3′ overhangs of double-strand breaks. SCAN1 cells deficient in TDP1 which have an inactivating mutation in the TDP1 active site Histidine residue were unable to process the substrates harboring 3′-PG moieties and this function was rescued by complementing the cells with recombinant TDP1 (Zhou et al. 2009). Apart from these blocks, TDP1 hydrolyses many other adducts that block the 3′ end of the DNA including AP sites and 3′-dRP ends. (Murai et al. 2012)
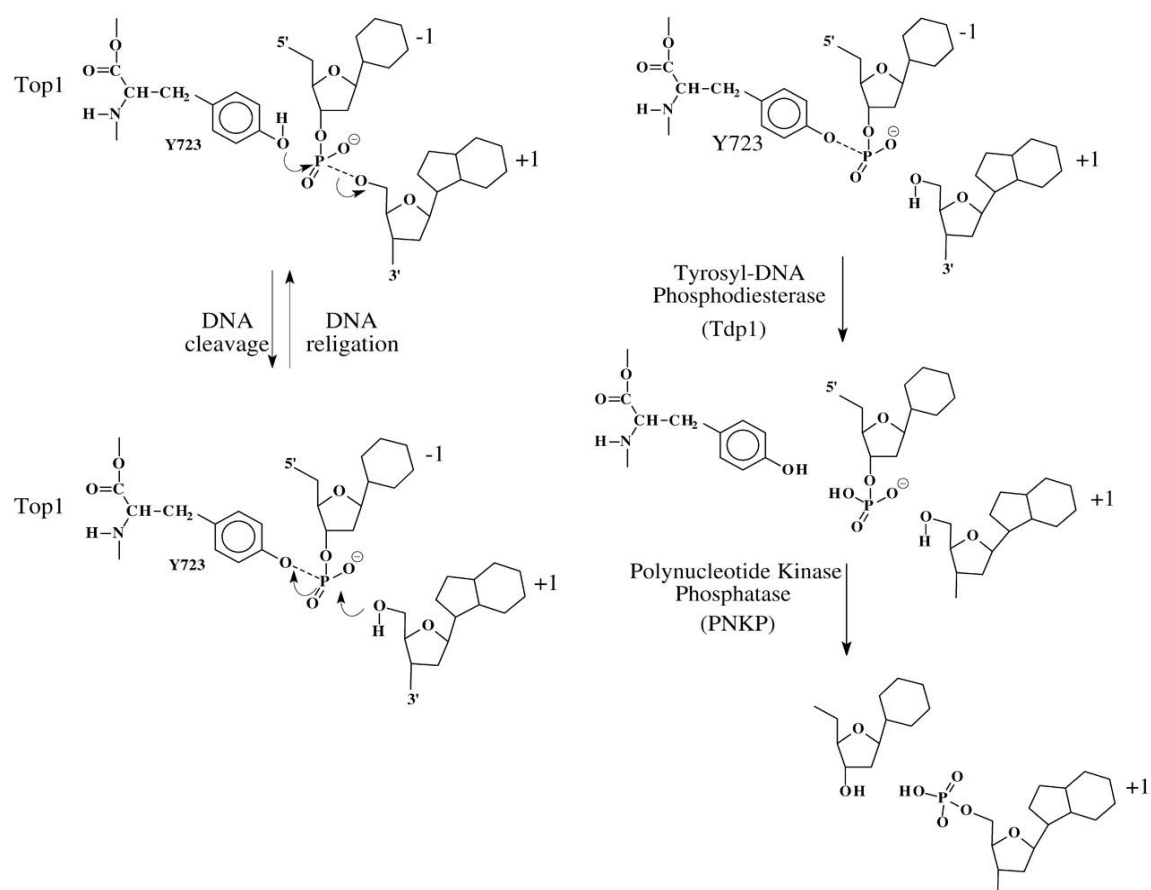
Figure 3 - Resolving TopI cleavage complexes by TDP1 and PNKP

The hydroxyl of tyrosine (Y723) of TopoI makes a nucleophilic attack on the phosphate of the

DNA phosphodiester backbone thereby covalently linking itself with the 3′-phosphate of DNA.

TDP1 releases the Tyrosyl moiety leaving a 3′-phosphate and a 5′-hydroxyl on the DNA.

Polynucleotide Kinase Phosphatase (PNKP) will then convert the ends to 3′-hydroxyl and 5′-

phosphate. (Debéthune, 2002)

1.3 Artemis:

Moshous and colleagues, first described a novel protein that was found to be involved in V(D)J recombination, while looking for a gene coding for a factor defective in human radiosensitive - severe combined immunodeficiency (RS-SCID), a disease which harbors symptoms of increased sensitivity to ionizing radiation (Li et al., 2002). In classical Greek mythology, Artemis was the goddess of protecting young children and as this condition was lethal within the first year of life of young children, the protein was named Artemis.

The gene encoding Artemis is DNA Cross-Link Repair 1C (DCLRE1C). Athabascan SCID or RS-SCID is a highly rare, autosomal recessive inherited disease which is characterized by early onset of severe opportunistic infections with severe oral and genital ulcers. Affected children generally die from these infections within six months without a bone-marrow transplant (Li et al, 2002). A unique, nonsense mutation in the DCLRE1C gene leading to the truncation of the protein product was also shown to cause SCID in Athabascan-speaking Native Americans (Li et al, 1998, Moshous et al, 2003).

Structure:

Artemis is a 78 kDa protein, coded from the short arm of chromosome 10, belonging to the metallo-β-lactamase family and consisting of 692 amino acids. Two domains in its N-terminus, a metallo-β-lactamase domain, spanning amino acids 1-155 and a β-CASP domain spanning amino acids 156-385, have been shown to be important for the catalytic activity of Artemis. The β-CASP domain is highly conserved in other proteins belonging to the same family that specifically act on nucleic acids. Like all proteins belonging to metallo-β-lactamase superfamily, Artemis also needs divalent cations, specifically Mg^{+2}, to be catalytically active (Pannicke et al. 2004). The active site

of Artemis contains 4 Histidine residues and 5 Aspartic acid residues which are highly conserved between Artemis and other metallo-β-lactamase proteins. These active site histidines and aspartates are thought to co-ordinate metal ions for a nucleolytic attack onto the DNA (Pannicke et al. 2004). The N-terminal region of Artemis is the catalytic region for the Artemis protein. The regulatory C-terminal region has been shown to be important for the interaction with DNA-PKcs. DNA-PKcs phosphorylates Artemis in its C-terminal region and causes a conformational change resulting in its activation.

Function

Artemis is the nuclease required for the resolution of the hairpin intermediates during the process of V(D)J recombination. In vitro studies have shown that DNA-PK phosphorylates Artemis and activates its hairpin loop opening function as cells deficient in DNA-PK fail to cleave the hairpin loop (Goodarzi et al., 2006). Artemis has an innate 5′ to 3′ exonuclease activity which is specific to single-strand DNA. However, upon phosphorylation by DNA-PK, its endonuclease function is activated (Kurosawa & Adachi, 2010).

Cells deficient in NHEJ proteins including DNA-PK show intensive radiosensitivity as do Artemis-defective cells, thus giving evidence to the requirement of Artemis in the NHEJ pathway for the repair of DSBs. Ionizing radiation, and radiomimetic drugs like Neocarzinostatin (NCS) create chemically modified, unligatable DSB ends, e.g. 3′-phosphates and 3′-phosphoglycolates. As Artemis-deficient cells are sensitive to IR, it was postulated that Artemis could mediate the end-processing of these chemically modified termini. Indeed, biochemical analysis have shown that Artemis in association with DNA-PKcs can convert such unligatable ends to a form that is appropriate for ligation with a minimal loss of the terminal nucleotides (Kurosawa & Adachi,

2010. Generation of blunt ends or 3′ overhangs of around 2-4 bases by the Artemis/ DNA-PKcs complex have further strengthened its role as an end processing enzyme in NHEJ.

Apart from its end-processing function, Artemis also plays a role in DNA damage signaling. ATM and Artemis deficient cells exhibit similar radiosensitivity and thus it was proposed that Artemis and ATM function in a common pathway (Riballo et al. 2004). Several studies on the role of Artemis in cell cycle progression have been carried out since then. Contrasting conclusions have been presented on its role in G2/M cell cycle checkpoint wherein one group reported a normal functional G2/M checkpoint in response to IR in Artemis deficient cells, thus revealing a prolonged G2/M arrest (Zhang X, *et al* 2004) while another group showed that Artemis deficient cells exhibit a defective recovery from this checkpoint which demonstrates that Artemis was required for G2/M arrest post IR treatment (Geng, Zhang, Zheng & Legerski, 2007). ATM hyperphosphorylates Artemis in response to IR treatment and thus ATM is required for Artemis-dependent processing of damaged DNA ends. ATM, however, is not required for V(D)J recombination activity of Artemis as A-T cells deficient in ATM are proficient in V(D)J recombination.

1.4 Ionizing radiation

The energy transmitted via X-rays, gamma rays, beta particles (high-speed electrons), alpha particles (the nucleus of the helium atom), neutrons, protons, and other heavy ions is defined as ionizing radiation. X rays and gamma rays are electromagnetic waves like light, but their energy is much higher than that of light. (Han W, 2010)

Ionizing radiation involve high energy particles travelling at an expeditious speed. When IR bumps onto molecules in the cell, it transfers its energy onto the electrons of that atom, thereby causing the release of the electrons from the atom and ultimately leading to the production of radicals.

Ionizing radiation (IR) interacts critically with a variety of biomolecules in the cell but the most harmful effects are as a result of triggering DNA damage. This damage can be direct when IR targets DNA directly causing damage to the phosphodiester backbone or indirect when radiation interacts with other molecules in the cell like water, leading to the production of a large number of free-radical species, including activated oxygen radicals, that may result in critical damage to targets within their diffusion distance. The damage inflicted by IR involve single-strand breaks, double-strand breaks, base damage and crosslink formation between DNA and proteins leading to stalled tertiary structures (Su, 2010). SSBs and DSBs are produced in different proportions in the cell. While there are 1000 SSBs estimated for a Gy of radiation, about 40 DSBs occur per diploid cell per Gy. (Ward, 1990)

1.5 Radiomimetic Agents

The idea of treating cancer through chemotherapy brought forth many anti-tumor antibiotics that target the DNA by inducing DNA damage (Dedon & Goldberg, 1992). These chemical agents induce free-radical based single- as well as double-strand breaks in the DNA molecule by attacking the deoxyribose moieties in the DNA phosphodiester backbone. Since their effects mimic that of ionizing radiation, these chemotherapeutic agents are termed as radiomimetic drugs. Although the action of these radiomimetic agents is highly specific, forming lesions which represent a subset of the lesions generated due to IR, the effect of IR and radiomimetic agents on cells is surprisingly similar.

Significant work has been published on some radiomimetic drugs like Bleomycin, Neocarzinostatin and Calicheamicin. Bleomycins are a family of glycopeptides first isolated from *Streptomyces verticillus* by Umezawa and colleagues in 1966 (Umezawa et al 1966). Since their

discovery, the bleomycins have been an important component in a number of combination chemotherapy protocols against testicular cancer (Einhorn, 2002) and certain types of lymphoma (Bayer et al 1992; Chen & Stubbe, 2005)

Neocarzinostatin and Calicheamicin are compounds which belong to the bicyclic enediyne family of anti-tumor antibiotics and are amongst the most studied of the radiomimetic drugs. These agents have a 10-membered characteristic unsaturated core containing two acetylenic groups conjugated to a double bond. These drugs are unique for their potential to produce sequence-specific double-stranded lesions which transpire due to the action of carbon-centered radicals of a single drug molecule (Dedon & Goldberg, 1992). Treatment of DNA with NCS in the presence of glutathione led to formation of double-strand breaks in a very high proportion with the ratio of single-strand lesions: double-strand lesions being around 2:1. The reaction of DNA with Calicheamicin was even more potent producing single-strand lesions: double-strand lesion ratio of around 1:20. (Chaudhry et al. 1999)

Both bleomycin and the enediyne neocarzinostatin (NCS) are potent clastogens, and they can also induce, in various systems, base substitutions small deletions and large-scale gene rearrangements, with reasonable efficiencies. That these mutations seem to so rarely result in carcinogenesis is certainly one of the most intriguing aspects of the genetic toxicology of these agents (Povirk, 1996).

Neocarzinostatin (NCS)

NCS was the first of the bicyclic enediyne antibiotics that was discovered. It was isolated from the bacterial species *Streptomyces carzinostaticus.* It was recognized as a simple antitumor antibiotic protein competent in inhibiting DNA synthesis and inducing the degradation of DNA in cells.

However, only 15 years after its discovery it was realized that the true biological function of NCS was not due to the protein but rather to a previously unrecognized tightly, but non-covalently, bound labile non-protein chromophore (NCS-Chrom). The apoprotein contains a hydrophobic cleft where NCS-Chrom is believed to reside and is protected from degradation. The structure of NCS can be divided into 3 domains, the naphthoate region which serves as the DNA binding domain, the enediyne core which form the DNA-damaging machinery and cyclic carbonate structure responsible for uptake of the drug in the cells (Dedon, P., & Goldberg, I. 1992).

The interaction of NCS with DNA has been extensively characterised. The drug binds to the DNA in a two-step process involving external binding followed by the intercalation of the chromophore. Electric dichroism studies have shown that the naphthoate acts as a classic intercalator, orienting itself parallel to the DNA bases which causes a distortion of the DNA helix (Dasgupta & Goldberg, 1985; Povirk, 1996) This leads to the positioning of the active enediyne portion of the NCS-chromophore in the minor groove of the DNA molecule with favourable electrostatic interactions between the positively charged amino sugar in NCS and the negatively charged Phosphodiester backbone. This binding of the drug in the minor groove is evident from 2 sources: Modification of the major groove did not alter the binding constant of NCS whereas Netropsin and distamycin, two minor groove binding agents competed with NCS for binding to DNA (Dasgupta and Goldberg, 1985)
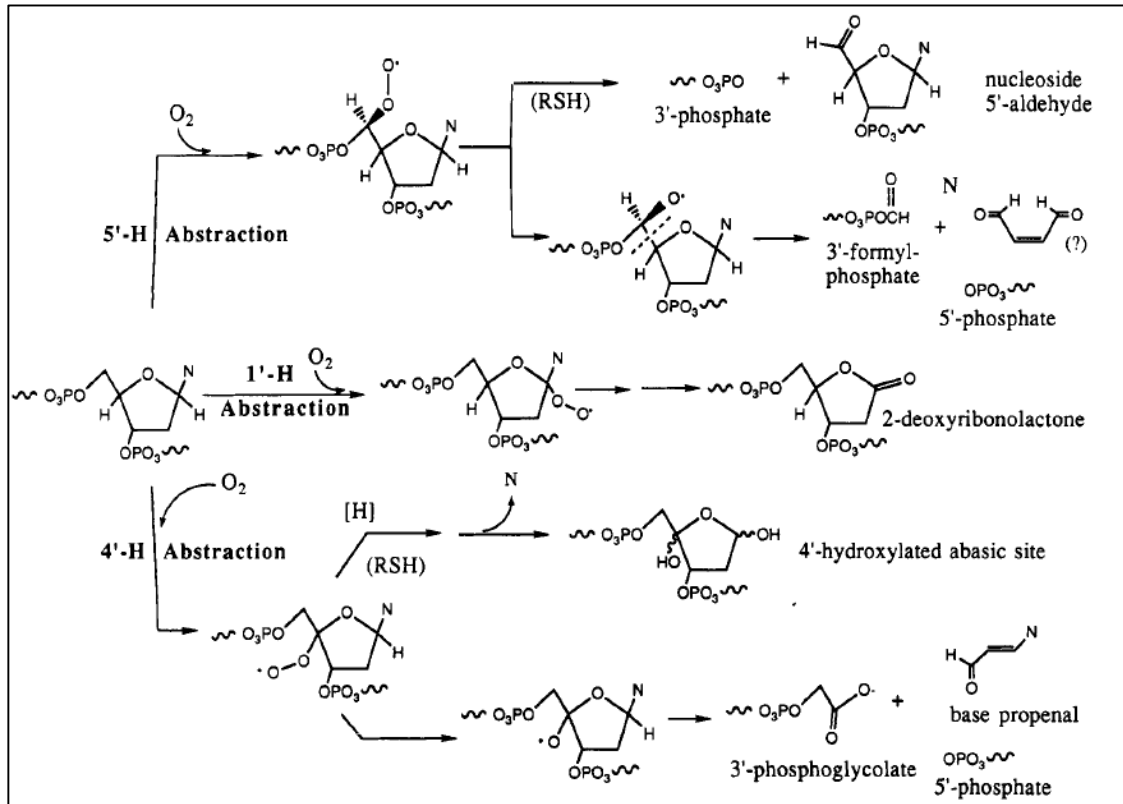
Figure 4 - Mechanism of Action of NCS and the typical DSB ends formed

NCS-mediated hydrogen atom abstraction can take place from 1′, 4′ or 5′ carbon of the deoxyribose sugar. 5′-H abstraction followed by oxidation leads to the production of 3′-phosphate and a nucleoside 5′-aldehyde in presence of thiols whereas in absence of thiols, 3′-formyl-phopshate and 5′-phosphate are formed. 1′-H abstraction leads to the formation of an abasic site and a 2-deoxyribonolactone. 4′-H abstraction, in the presence of thiols, leads to the formation of a 4′-hydroxylated abasic site whereas in the absence of thiols, 3′-phosphoglycolate and a 5′-phosphate are formed with the release of the base propenal (Dedon & Goldberg, 1992).

Mechanism of Action:

The mechanism of action of NCS and the damage caused by it is highly complex. NCS-mediated DNA damage results in the formation of single as well as double-strand breaks. Similar to all radiomimetic drugs, its mechanism of action is based on the hydrogen atom abstraction principally at the 1st, 4th and 5th carbon of the deoxyribose sugar leading to its oxidation (Povirk and Steighner. 1989). The identity of these hydrogen atoms abstracted have been verified using isotope labelling studies (Dedon & Goldberg, 1992). Abstraction of the hydrogen from the C-5′ end is the characteristic trait of the enediyne compounds resulting in the formation of a 3′-phosphate and a 5′-aldehyde molecule at the DNA terminus (Kappen et al., 1982). A small subset of breaks also involves 3′- and 5′- phosphates at the termini as well. This hydrogen abstraction from the 5th carbon of the deoxyribose sugar followed by the incorporation of oxygen into the aldehyde leads to the production of single-strand breaks in the DNA strands.

In contrast to the above mechanism, hydrogen abstraction from both C-1′ and C-4′ leads to the formation of bi-stranded lesions. Elimination of the C-1′ hydrogen by NCS mainly results in the formation of an abasic site in the form of 2′-deoxyribonolactone. This species is quite unstable in alkali and ultimately leads to the formation of a strand break with 3′- and 5′-phosphate termini. (Povirk and Houlgrave, 1988; Povirk et al. 1988). NCS-mediated attack at C-4′ adds oxygen at C-4′ ultimately leading to the production of strand breaks with ends containing 3′-phosphoglycolates and 5′-phosphates with the formation of a base, propenal (Chaudhry et al, 1999).

Figure 5 - Structures of Enediyne antitumor antibiotics: Calcheamicin γ1 and Neocarzinostatin (Dedon & Goldberg, 1992).
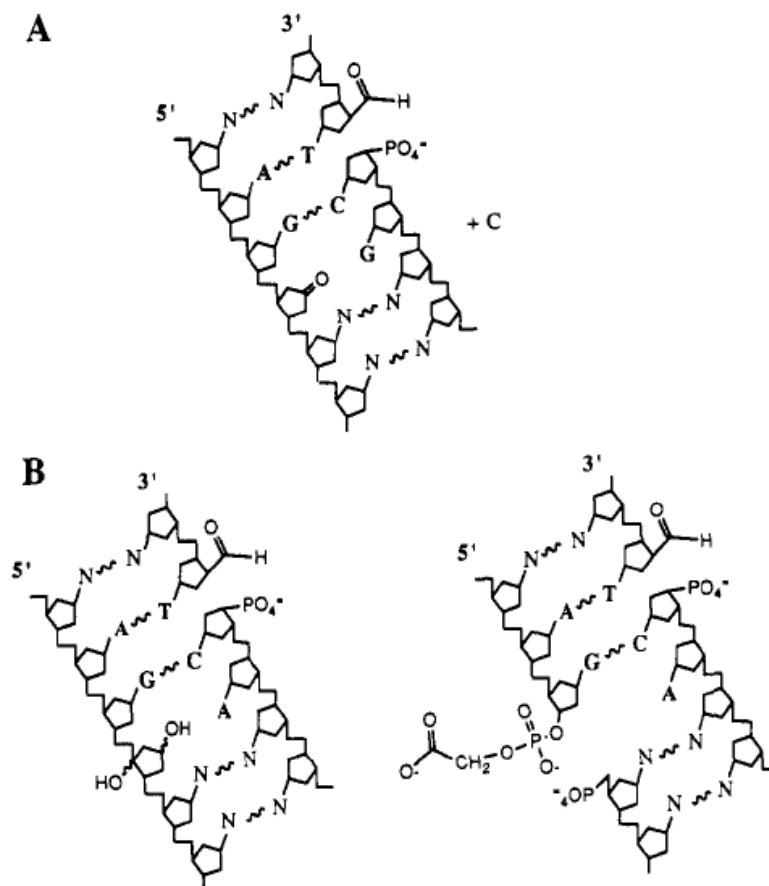
Figure 6 - Models of NCS-induced bi-stranded lesions

NCS has been shown to produce two types of bistranded lesions: **A**. At the AGC.GCT sequence in Fig. 6 (A), C1′-hydrogen abstraction at the C of AGC along with the C5′-hydrogen abstraction at the T residue of the complementary strand leading to the formation of an abasic site instead of the C residue and a 3′-phosphate on the other strand. **B**. At the AGT.ACT sequence, bistranded lesions consists of mainly C4′ -hydrogen abstraction at the T of AGT, as suggested by the presence of 3′-phosphoglycolate residues and 4′ -hydroxylated abasic sites, and C5′-aldehyde at the T of ACT (Dedon & Goldberg, 1992).

Calicheamicin

The calicheamicins are produced by the fermentation of *Micromonospora echinospora ssp calichensis*, a bacterium isolated from a chalky, or caliche, soil sample collected in Texas. They were discovered in the mid- 1980s in a fermentation products screening program through the use of the biochemical induction assay (BIA), which utilized a genetically engineered strain of Escherichia coli to detect DNA damaging agents (Lee et al 1991).

Calicheamicin and Esperamicin lack intercalating moieties and thus bind to DNA by other means than NCS. The carbohydrate side chains of Calicheamicin serve as a DNA binding domain. The DNA damaging element present in Calicheamicin is similar to NCS consisting of a highly strained ring system with a pair of triply unsaturated carbon bonds surrounding a carbon-carbon double bond (Lee et al 1991).

The nature of DNA damage instigated by Calicheamicin has not been as extensively studied as some of the other enediynes like NCS. However, it is known to produce both single- as well as double-strand lesions with an astoundingly high proportion of double-strand lesions (Dedon & Goldberg, 1992).

1.5 Epistasis:

Cells are under constant abuse from the environment and undergo tremendous amount of DNA damage and as such have evolved important repair pathways in order to repair the damage. One of the principal question in the field of DNA damage is to understand which of these DNA repair proteins (enzymes) function together in a common, specific DNA repair pathway. Modern genetic approaches have enabled researchers to answer these questions through a variety of means. One way is to create a mutant strain absent in individual repair proteins and to observe the phenotypic

effect of the mutation. Subsequent generation of double mutants would lead us to observe if the system behaves in a similar way or if the phenotype worsens.

If the phenotype of the double mutants is not worse than that of the single mutants, the two repair proteins are said to exhibit an epistatic relationship with each other. In the simplest mechanistic model, such epistasis suggests that the proteins each perform different essential function in the same repair pathway. On the other hand, if the double mutants manifest a worsened phenotype as compared to the single mutants, they are thought to be synthetically lethal or synergistic. Mechanistically, this is the result expected if the two proteins are a part of two alternative pathways of resolving the same DNA lesion.

1.6 Specific Purpose:

Artemis and TDP1 are alternative end processing enzymes involved in DNA repair. shRNA mediated knockdown of TDP1 and Artemis knockout results in sensitivity to NCS and Calicheamicin, drugs that produce 3′-phosphoglycolate-terminated double-strand breaks. In order to further explore the role of TDP1 in NHEJ and its possible interplay with Artemis, an HCT116 derivative cell line double deficient in Artemis and TDP1 was created followed by the assessment of growth rates, cell cycle profiles, DNA repair ability and survival of these cell lines in response to radiomimetic agents.

2. MATERIALS AND METHODS

2.1 Cell Lines and Cell culture

The tumour cell lines used in this study were human colon adenocarcinoma cell line HCT116 and its derivative cell lines involving knockdown of TDP1 (HCT116 shTDP1), knockout of Artemis (HCT116 Art-/-) (obtained from Dr. Eric A. Hendrickson, University of Minnesota) and a combined deficiency exhibiting knockout of Artemis and knockdown of TDP1 (HCT116 Art-/- .shTDP1). All cell lines were cultured in 10cm dishes, in 10 mL Roswell Park Memorial Institute (RPMI) 1640 medium (GIBCO) with 10% Fetal Bovine Serum (FBS) and 1X Penicillin/Streptomycin which was referred to as complete medium and maintained at 37°C in 5% CO_2 atmosphere. After the cells had attained around 85-90% confluency, they were harvested in complete medium with 10% DMSO in a total volume of 1mL in cryogenic vials. These cryogenic vials were frozen slowly at -80°C for one day and then transferred to liquid nitrogen where it was stored for long periods at -196°C. A new vial of every cell line was thawed for each experiment.

2.2 Knockdown of TDP1

For the expression of TDP1 shRNA, we used the pLSLPw lentiviral vector, a distant relative of the pLV vector that contains an RNA polymerase III-driven H1 RNA promoter controlling the expression of a hairpin shRNA transcript and harbors the puromycin N-acetyl transferase (*pac*) gene which confers resistance to the antibiotic puromycin. (See Supplemental Material from Budanov et al., 2004)

The phosphorylated oligomers GATCCGGTGATAAGCGAGAGGCTAACTTCCTGTCAT TAGCCTCTCGCTTATCACTTTTTG and AATTCAAAAAGTGATAAGCGAGAGGCTA ATGACAGGAAGTTAGCCTGTCGCTTATGACCG were annealed and cloned into the BamHI and EcoRI sites of the dephosphorylated vector, pLSLPw. This vector expresses a hairpin that targets the sequence GUGAUAAGCGAGAGGCUA (bases 20300-20319 in exon 6 of the TDP1 gene, GenBank #NG009164). (See Supplemental Material from Akopiants et al., 2014). The vector was co-transfected along with packaging plasmids pLP1, pLP2 and pLP-VSVG into HEK293T cells with Lipofectamine 2000 (Invitrogen). Medium containing packaged lentivirus was collected 48 hour post tranfection and was centrifuged for 5 min at 1200 rpm at room temperature. The supernatant was filtered through 0.45µm filter (Novagen), followed by ultracentrifugation of the sample at 20,000 rpm for 2.5 hour at 4°C in a SW28 rotor (Beckman). Resulting viral pellets were resuspended with 200µL of Hanks balanced salt solution and stored in 10µL aliquots at -80°C. HCT116 and HCT116 Art-/- cells were seeded in 25cm dishes and incubated for 24 hour. Once they had attained around 80% confluency, they were infected with 5µL of concentrated lentivirus with 4µg/mL polybrene in 1mL medium without serum for 8 hour, then fed with fresh medium and incubated for 48 hour. Cells were then selected in 0.8µg/mL Puromycin for 96 hours. Cells were expanded under selection to produce cryogenic stocks. Genomic DNA was isolated from 1

million cells using the QIAGEN DNeasy Blood and Tissue Kit in order to genotypically screen these cells for stable integration of the Puromycin N-Acetyl Transferase (Pac) gene. Genomic DNA (100ng/µL) was used as template to amplify the gene by Polymerase Chain Reaction (PCR). The primers used were: Forward: 5′-CGAGTACAAGCCCACGGT-3′, Reverse: 5′-AGACCCTTGCCCTGGTG-3′ (synthesised by IDT) with initial denaturation at 94°C for 6 min followed by cycles of denaturation at 94°C for 10 sec, annealing at 54°C for 20 sec and extension at 72°C for 30 sec for 35 cycles, followed by a final extension step at 72°C for 7 min. Following PCR amplification, samples were separated on 1% agarose gel to confirm the presence of the gene.

2.3 Selection of clones:

From the puromycin-selected cells, 5 cells were seeded in 15mL complete medium in 15 cm dishes and the cells were made to form colonies over a period of 14 days. Following colony formation, the medium was removed and the colonies were washed with 5mL of PBS. A sterile ring was placed on top of the colonies and 70µL trypsin was added in each ring to dissociate the cells. The trypsinized cells were sub-cultured into individual 10 cm dishes to obtain individual clones. From the puromycin-selected cells, 13 clones were obtained by this method in order to obtain a homozygous population of these cells.

2.4 TDP1 Activity Assay

The enzymatic activity of TDP1 in the individual clones was assayed to identify the clones with maximum TDP1 knockdown. A 5′-Cy5-labelled 18-base oligonucleotide with the sequence TCCGTTGAAGCCTGCTTT with a Tyrosine residue covalently linked to its 3′ -end, purchased from Midland Certified Reagent, Midland, TX was used as a substrate in this enzyme assay (Yang,

S. et al 1996). Whole-cell extracts were prepared by harvesting one million cells and lysing them using 100 µL of KV Lysis Buffer (10mM HEPES at pH 7.8, 60mM KCl, 1mM EDTA, 0.5% NP-40) in presence of 0.5 mM serine protease inhibitor phenylmethanesulfonyl fluoride (PMSF) plus (1mM $NaVO_4$, 1µg/mL leupeptin, 1µg/mL aprotinin and 1µg/mL pepstatin) which is commonly used in the production of cell lysates. The lysed cells were placed on ice for 5 min and then centrifuged at 13000 rpm for 5 min at 4°C. The supernatant, obtained as cell extract, was collected in different tubes. The extracts from the control cells (HCT116 Art-/-) were serially diluted 1, 25, 125, 625, 3025 times while the mutant HCT116 Art-/-.shTDP1 cell extracts were diluted 1, 5, 25, 125, 625 times in Pouliot dilution buffer (50mM Tris at pH 8.0, 5nM DTT, 100 mM NaCl, 5mM EDTA, 10% glycerol, 500µg/mL BSA). The substrate was added at a final concentration of 4pM to the diluted tubes to a total volume of 5µL and the reaction performed at 37°C for 1 hour in 1X Kedar Buffer (60mM K-acetate, 10mM Mg-acetate, 50mM Triethanolamine-HAc pH 7.5, 2mM ATP, 1mM DTT). This was followed by quenching of the reaction at 95°C for 1 min. SGLS (5µL) (98% Formamide, 20µM EDTA, Bromophenol Blue) was added in every sample. The samples were then analysed by Polyacrylamide Gel electrophoresis.

Total Protein in these whole-cell extracts was estimated by Bradford's Assay (Bradford, M. 1976). Standard protein used was 2mg/mL BSA to obtain the standard curve.

2.5 Polyacrylamide Gel Electrophoresis

Denaturing polyacrylamide gels with acrylamide: bisacrylamide ratio of 20:1 and Urea at a final concentration of 8M were used for separation of the oligonucleotide substrate with and without the Tyrosyl attached to its 3′ -end. The gel dimensions were 33cm X 38cm X 0.1cm. Urea was dissolved into the mixture before adding 0.075% ammonium persulfate and 0.0625% TEMED (N',

N', N', N'-tetramethylethylene diamine). The gel was allowed to set for around 1 hour, following which the samples were loaded into the wells of the gel and electrophoresed at constant power of 60W for around 4 hours in 1X TBE buffer (10X stock solution: 108 g of Tris base, 55g of boric acid, 9.3g of disodium EDTA in 1L Distilled water). The gel was wrapped in saran wrap following electrophoresis and scanned on a Typhoon 9410 Variable Mode Imager in Fluorescence Acquisition mode with 670BP 30 Cy5 Emission filter using a Red (633) laser at photomultiplier tube voltage of 800 V.

2.6 Clonogenic Survival Assay

All the four cell lines were harvested from exponentially growing cultures. They were counted using a hemocytometer and plated in 60 mm dishes in 4mL complete medium ranging from 300/plate to 10000/plate. After 16 hours, the cells were treated with 0.25, 0.5, 1 or 2nM NCS (stock concentration 2µM diluted in 20mM sodium citrate at pH 4.0) for 6 hours. For the experiments in which Calicheamicin was used as a radiomimetic agent, the cells were treated with 0.3, 0.6, 1.2 or 2.4pM (stock concentration 20µM Calicheamicin diluted to 1µM in 50% Ethanol, further diluted in PBS to obtain final working concentration of 1.2nM) for 24 hours. Following treatment, the medium was removed, cells washed with PBS and allowed to form colonies in complete medium for a period of 9 - 13 days. Following this, the medium was removed and colonies were washed with 5 mL PBS. They were later fixed in 100% Methanol for 10 min, stained with 0.5% Crystal Violet for 10 min and washed with distilled water. The plates were allowed to air-dry and the colonies were counted manually. Plating Efficiency (PE) was defined as the number of colonies counted/ the number of cells seeded. The survival fraction (SF) of untreated cells was defined as 100. SF was calculated as PE treated/ PE untreated * 100.

2.7 Immunofluorescence Microscopy

All four cell lines were counted using a hemocytometer and 15000 cells were grown on 4-well chamber slides (Nunc lab tek). After attachment, the cells were serum starved for 48 hours, following which they were either immediately processed; treated with 4nM NCS for 1 hour and then processed or treated with 4nM NCS for 1 hour and then allowed to repair the damage by releasing in serum for 8 hours prior to processing. After the treatments, the medium was removed and the cells were washed twice with phosphate-buffered saline (PBS). Cells were immediately fixed with 3% paraformaldehyde for 15 min at room temperature. The excess of paraformaldehyde was washed away with PBS and then the fixed cells were permeabilized with a permeabilizing solution (0.5% Triton X-100 in PBS) for 10 min. After washing away the excess of permeabilizing solution, cells were then treated with Blocking solution (5% FBS in PBS) for 2 hours at room temperature. The blocking solution was removed and they were then incubated with 0.3mL of anti-53BP1 mouse primary antibody (a gift of Dr. David Gewirtz, Virginia Commonwealth University, originally from Dr. Thanos Halazonetis, University of Geneva) at 1:250 dilution overnight at 4°C. After washing 4 times with PBS for 15 min, the cells were incubated for 3 hour with 0.3 mL secondary goat anti-mouse Alexa Fluor 488 antibody (*Life Technologies*) at 1:500 dilution at room temperature. The excess antibodies were washed with PBS and then the cells were fixed with 3% formaldehyde. The nuclei were counterstained with VECTASHIELD Mounting medium with 1.5 µg/mL 4′ -6-diamidino-2-phenylindole (DAPI) (Vector Laboratories Catalog # H-1200) having a refractive index of 1.45. Immunofluorescence was observed with the Zeiss LSM700 Confocal Laser Scanning Microscope and confocal images were obtained using a 430-nm diode laser with a 605-nm band pass filter (DAPI), a 510-nm laser with a 530-nm band pass filter (Alexa Fluor

488). Foci from around 100 cells were counted manually for each condition in 3-4 different experiments for each cell line.

2.8 Cell Cycle Analysis by Flow Cytometry

All the four cell lines were seeded at a density of 5×10^5 cells/ dish in 100mm tissue culture dishes and cultured in complete medium. After 24 hours, the medium was removed and cells were synchronised by serum starving them in medium containing 0.5% FBS for 96 hours. Cells were either treated or not treated with 4nM NCS for 1 hour. Following treatment, the medium was changed, cells were washed with PBS and released in serum for different time points including 10, 12 and 14 hours. At the prescribed time points, the medium was removed, cells were washed with PBS twice and trypsinized. 1.5 X 10^6 cells were then counted using a hemocytometer and centrifuged at 800 rpm for 5 min. The pellets were resuspended in 1.5 mL Propidium Iodide (PI) solution (3.8mM Sodium Citrate, 0.05mg/mL PI, 0.1% Triton X-100). 10μL of RNase B at a final concentration of 7000units/mL was added to the above solution. The samples were stored overnight in dark at 4°C in 5mL Polystyrene Round-Bottom Tube with Cell-Strainer Cap (Fisher Scientific). Cells were processed for Flow Cytometry analysis after either 24 hours of culture, 96 hours of serum starvation or at the mentioned time points with or without the drug treatment. Cell Cycle Analysis was performed using a Becton Dickinson (San Jose, CA) FACS Canto II flow cytometer. The argon ion laser set at 488 nm was used as an excitation source. Cells having DNA content 2N were designated as being in the G1 phase of the cell cycle, those having 4N were designated as being in the G2 phase while the cells showing intermediate DNA content between 2N and 4N were designated as S-phase cells. Ten thousand events were acquired for each sample and the data obtained was analysed using the Modfit LT software.

2.9 Statistics:

Error bars represent standard error of mean (S.E.M) for at least 4 independent experiments. Graphical analysis was performed using SigmaPlot 12.5 statistical software. Unpaired two-tailed t-tests were performed using GraphPad QuickCals software.

3. RESULTS

3.1 Generation of a derivative cell line with double deficiency in Artemis and TDP1:

In order to understand the relationship between Artemis and TDP1, we created human colon adenocarcinoma HCT116 derivative cell lines with a double deficiency in Artemis and TDP1. HCT116 cells deficient in Artemis (HCT116 Art-/-) were obtained as a generous gift from Dr. Eric A. Hendrickson, University of Minnesota. These HCT116 Art-/- cells were infected with a lentivirus expressing a TDP1 shRNA. This TDP1 shRNA was cloned into the BamHI and EcoRI sites of the transfer plasmid pLSLPw (Fig. 7) which also harbours the Puromycin N-Acetyl transferase (*pac*) gene which confers resistance to the antibiotic Puromycin (Sánchez-Puig & Blasco, 2000). Human cells are naturally devoid of this gene and thus are sensitive to Puromycin. Successful lentiviral integration was confirmed by culturing the infected cells in RPMI medium with 0.8μg/mL Puromycin for 4 days. The cells that had undergone this puromycin selection were further confirmed by performing a genotype analysis. Genomic DNA was extracted from 1×10^6 cells and was used as a template in a Polymerase Chain Reaction in order to amplify the *pac* gene. Genomic DNA from HCT116 WT cells, which were not infected with the lentivirus, was used as a negative control. A plasmid pTripz Tdp harboring the *pac* gene was used as a positive control. The band size obtained was about 550 bp which corresponds to the size of the *pac* gene on the plasmid pLSLPw (puro) (Fig 8).

Dilution cloning was performed on these selected cells in order to obtain individual clones. 13 clones were obtained following dilution cloning which were further assayed to analyse the clones with the maximum amount of knockdown of TDP1 expression.
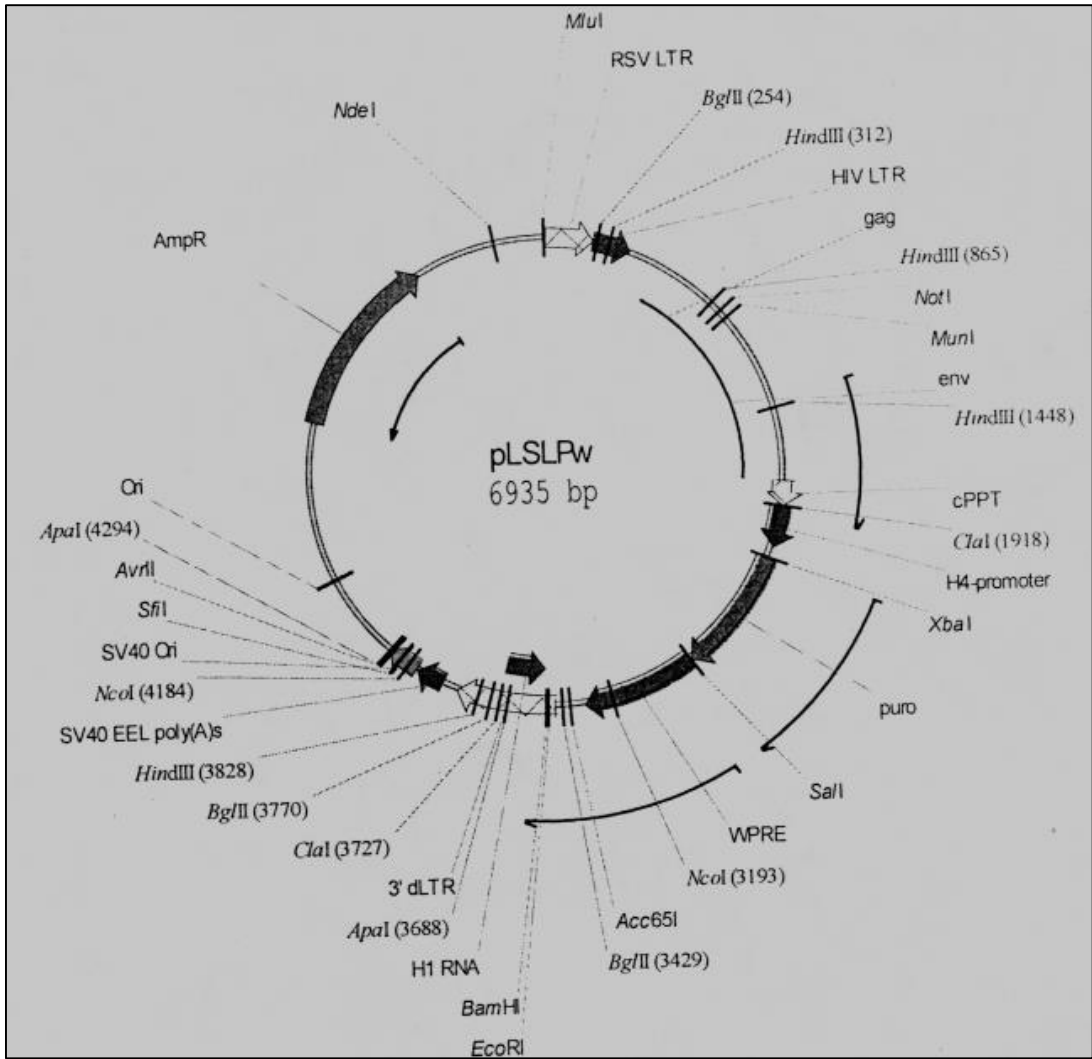
Figure 7 - Transfer plasmid pLSLPw

The shTDP1 construct was cloned into the BamHI and EcoRI sites seen at the bottom. The vector also carries a Puromycin N-Acetyl transferase (*pac*) gene seen here as puro on the right which confers resistance to the antibiotic puromycin. Successfully infected cells were rendered resistant to puromycin and thus were selected in medium containing 0.8μg/mL puromycin.
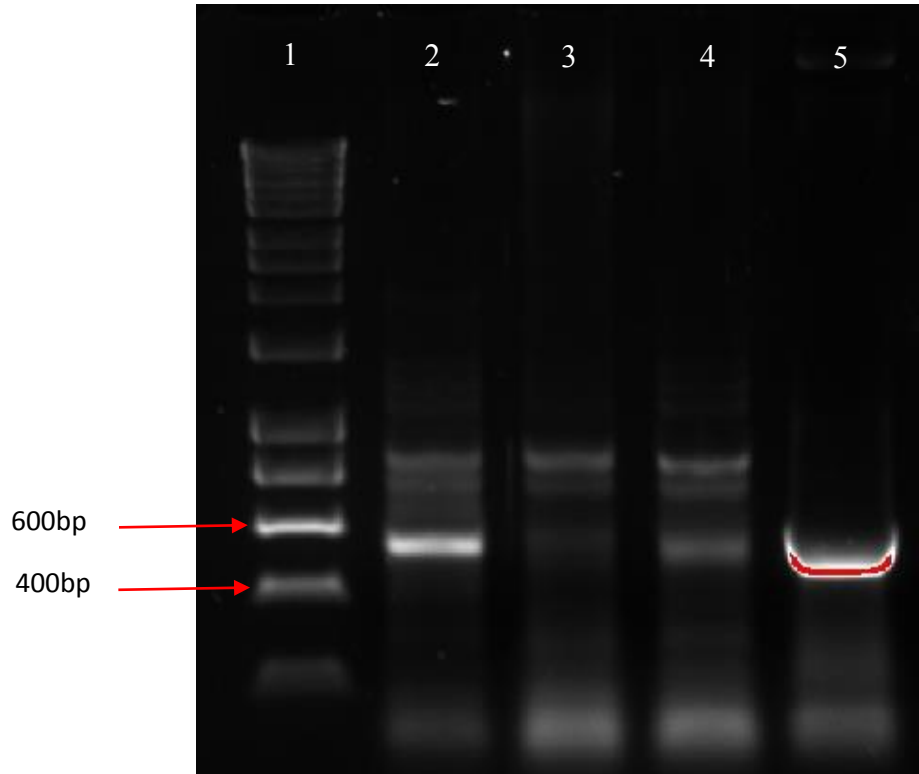
Figure 8 - Genotypic confirmation of lentiviral integration

Genomic DNA was isolated from 1 million cells of different derivative HCT116 cell lines as mentioned below:

Lane 1: DNA Hyperladder I (Bioline). Lane 2: HCT116 Art-/- cells transfected with the lentivirus carrying the shTDP1 construct. Lane 3: Negative control: Genomic DNA extracted from HCT116 WT cells and amplified using the same conditions. Lane 4: HCT116 cells infected with a lentivirus carrying another vector pTripz Tdp containing a *pac* gene was used as a positive control. Lane 5: Plasmid pTripz Tdp.

3.2 TDP1 Activity Assay:

During DNA replication, Topoisomerase I, through its Tyrosyl 723 residue, forms rare covalent complexes with the DNA which are referred to as Top1 cleavage complexes. TDP1 is the only enzyme known to remove these phosphotyrosyl residues from the 3′-end of the DNA. This attribute of TDP1 was utilised in order to assess the amount of knockdown achieved in the HCT116 Art-/- .shTDP1 individual clones by performing a TDP1 activity assay. Serially diluted whole-cell extracts from Art-/- and Art-/-.shTDP1 cells were incubated with an 18-base oligonucleotide containing a phosphotyrosyl moiety at the 3′-end. Extracts from cells expressing TDP1 would cleave the 3′-tyrosyl residue from the 18-base oligonucleotide substrate and form a product having a lower molecular weight than the substrate which would, migrate faster on a gel whereas extracts deficient in TDP1 would fail to cleave the 3′-tyrosyl residue on the substrate and thus the high molecular weight substrate migrate slower giving rise to a band above the band of the product. Fig. 9 shows the p-Tyr processing ability of 3 of the 13 double deficient clones. This activity of the clones was drastically hampered as compared to the Art-/- single mutant control cells. Table 1 shows the amount of knockdown achieved in all the double deficient clones with respect to the HCT116 Art-/- single mutant control cells. TDP1 activity titrations indicated a 12-fold decrease in the p-Tyr processing ability of Clone #7 thus manifesting the highest knockdown of TDP1 expression among all the other clones.

Bradford's assay was used to estimate total protein concentration in the whole-cell extracts. A standard curve was obtained by using 2mg/mL BSA. The extract concentrations of the control cell line (HCT116 Art-/-) and all the individual clones were in a similar range as can be seen from Table 1.
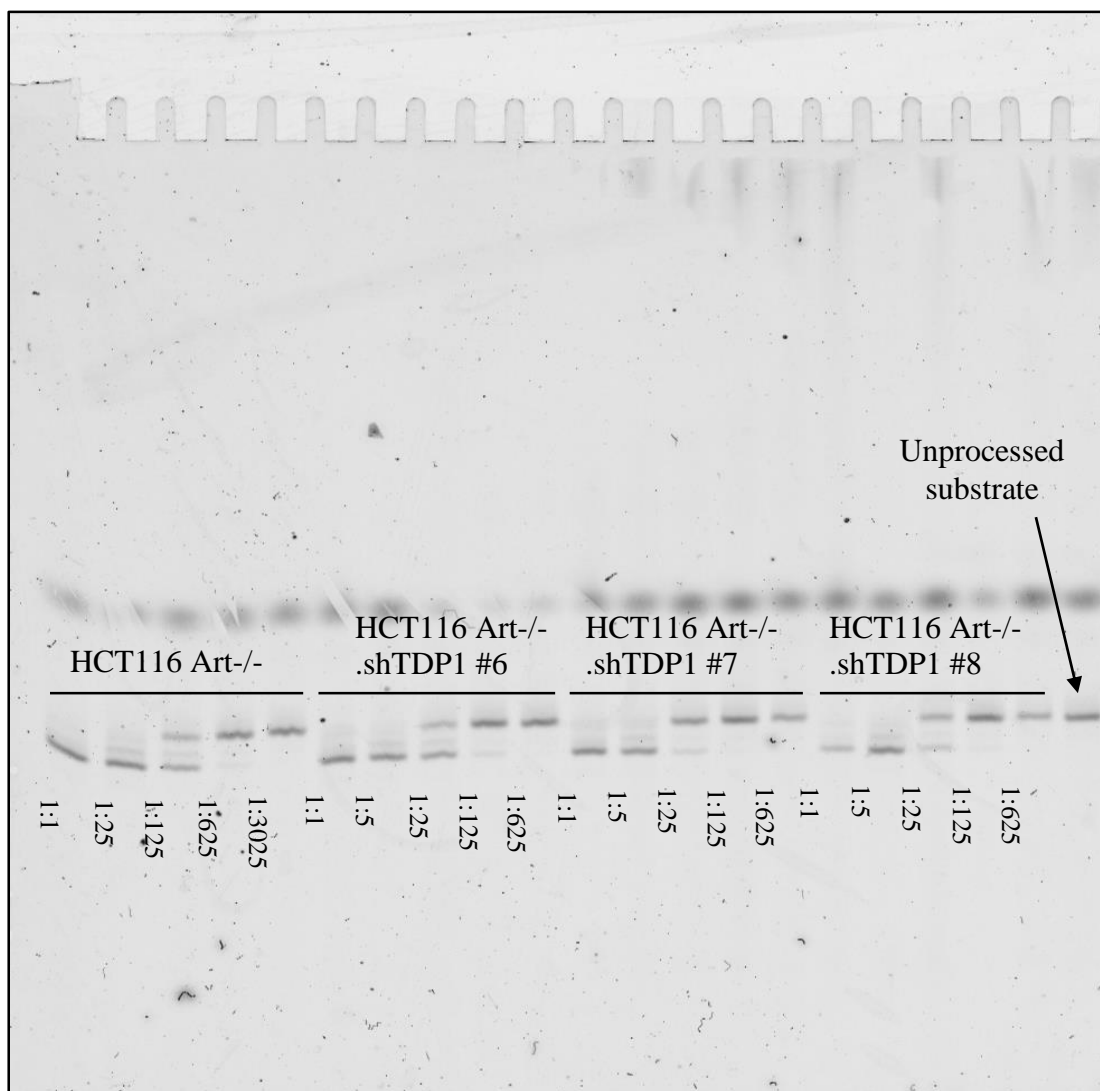
Figure 9 - TDP1 Activity Assay

Whole-cell extracts from HCT116 Art-/- cells and HCT116 Art-/-.shTDP1 individual clones were incubated with the 18-base 3′-tyrosyl linked oligonucleotide substrate at 37°C for 1 hr. The reaction was quenched at 95°C for 1 min and the samples were analysed on a 20% denaturing Polyacrylamide gel. The extracts and their dilution factors have been labelled. In the unprocessed substrate sample, the substrate was incubated with distilled water instead of cell extract and the reaction was performed in the same way as the other samples.

Standard Curve (BSA - 2mg/mL)

$R^2 = 0.9824$
$y = 0.039x$
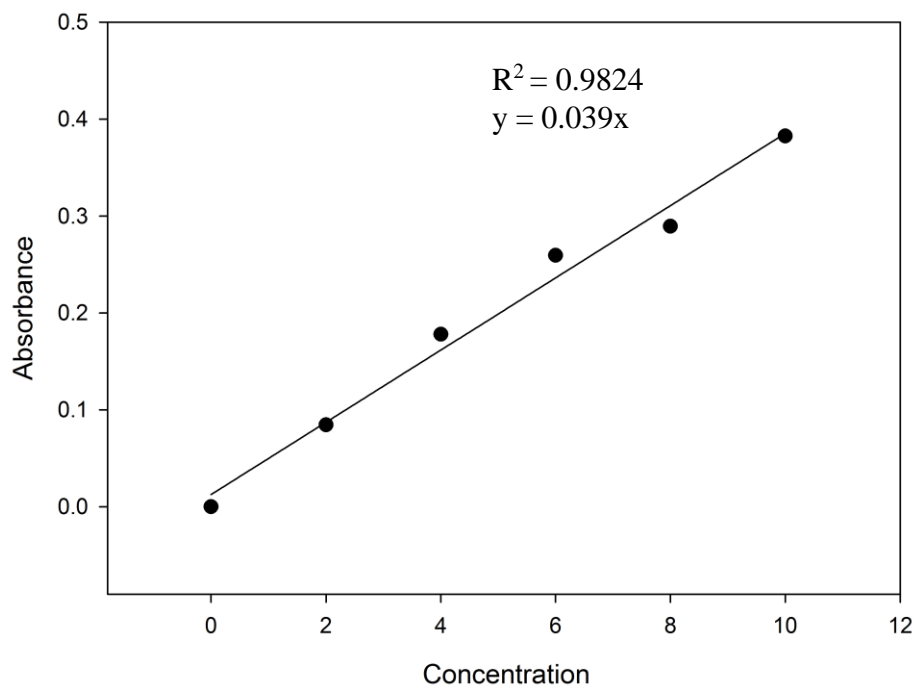
Figure 10 - Standard curve for estimating total protein concentration in cell extracts

R^2 value was obtained by regression analysis which was equal to 0.9824.
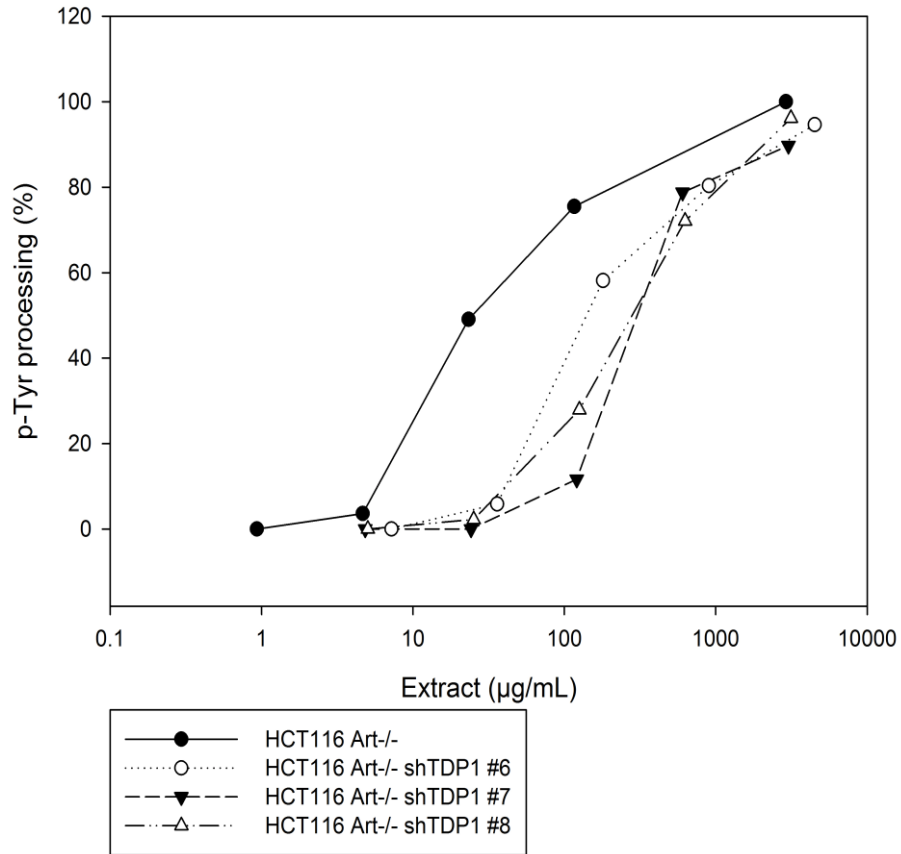
Figure 11 - Estimation of TDP1 Knockdown in HCT116 Art-/-.shTDP1 individual clones
Three out of the 13 clones are shown. Graph indicates p-Tyr processing (%) vs. concentration of extract in µg/mL.

Table 1 - Amount of Knockdown achieved in the HCT116 Art-/-.shTDP1 clones

Samples	TDP1 Knockdown (times Art-/-)
HCT116 Art-/-	-
HCT116 Art-/-. shTDP1 #1	1.44
HCT116 Art-/-. shTDP1 #2	6.92
HCT116 Art-/-. shTDP1 #3	5.25
HCT116 Art-/-. shTDP1 #4	6.3
HCT116 Art-/-. shTDP1 #5	6.3
HCT116 Art-/-. shTDP1 #6	5.75
HCT116 Art-/-. shTDP1 #7	12
HCT116 Art-/-. shTDP1 #8	11
HCT116 Art-/-. shTDP1 #9	2
HCT116 Art-/-. shTDP1 #10	1.4
HCT116 Art-/-. shTDP1 #11	3.7
HCT116 Art-/-. shTDP1 #12	4.2
HCT116 Art-/-. shTDP1 #13	8

3.3 Deficiency of Artemis and TDP1 causes an additive decrease in the growth rate

A cell is an intricate network with all processes working in concert to help it survive and grow. Thus, defect in some of these processes would compromise the overall growth of the cells. In order to observe if the above fact was applicable to our study, we performed a growth rate analysis of all the four cell lines. 1×10^5 cells were seeded in 6-well plates in 3mL complete medium. Cell counts after trypsinization were obtained using a hemocytometer for a period of 1 week.

As seen in Figure 12, the WT cells showed an exceptionally fast growth rate with a doubling time of around 14 hours. Artemis-deficient cells did not show a marked retardation in growth initially however, the sluggish growth rate was prevalent after a period of 6 days. The TDP1 deficient cells showed an opposite phenotype with retardation in growth initially followed by an increase in the growth rate around 6 days. The double mutant cells deficient in both Artemis and TDP1 showed prominent delay in growth with a doubling time of around 28-30 hours.
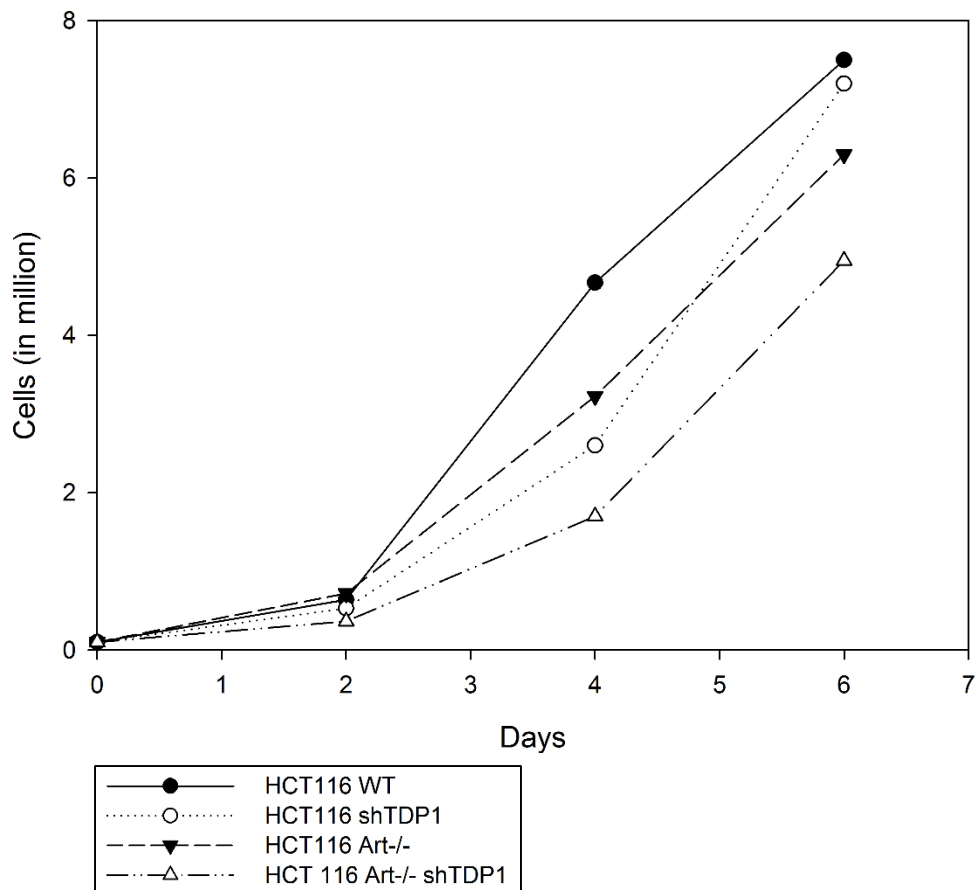
Figure 12 - Differential growth rate of all the cell lines

1×10^5 cells were seeded in 6-well plates in 3mL complete medium on day 0. Cells were counted using a hemocytometer on days 2, 4 and 6. The above graph shows the number of cells in million versus number of days.

3.4 Surprisingly, Artemis and TDP1 exhibit an epistatic relationship with each other:

TDP1 and Artemis are end processing enzymes involved in the removal of various 3′- and 5′-blocks. We wanted to investigate whether TDP1 and Artemis are alternative end processing enzymes functioning in the same pathway. Thus, in that effect, we carried out a pilot experiment in which a Clonogenic Survival Assay was performed on HCT116 Art-/- and HCT116 Art-/-shTDP1 #7 derivative cell lines.

Cells within a range of 300 – 10000 were plated in 6cm dishes. After 24 hours, the cells were treated with Calicheamicin, a radiomimetic drug which produces DSBs with 3′-phosphoglycolates ends, within a concentration range of 0pM - 2.4pM for 24 hours. The drug was removed and the cells were allowed to form colonies for a period of 12 days. Colonies were then fixed, stained and counted manually with a minimum of 50 cells constituting a colony. As seen in Fig. 13, surprisingly, there was no difference in sensitivities of the Art-/- single mutants as well as the Art-/-.shTDP1 #7 double mutants in response to Calicheamicin. Both cell lines showed similar percentage of survival indicating that Artemis and TDP1 could play a role in the same pathway and that TDP1 and Artemis exhibit an epistatic relationship. We wanted to further bolster this fact and confirm the epistatic relationship between Artemis and TDP1. To that effect, we performed Clonogenic Survival Assays with all the four cell lines, HCT116 WT and its derivative single mutants cell lines Art-/-, shTDP1 and the double mutant cell line Art-/-.shTDP1 in response to Neocarzinostatin, another radiomimetic drug that produces DSBs with 3′-phosphoglycolate ends. Fig 14 shows the sensitivity of these cell lines as percentage of cell survival after treating the cells with concentration of NCS ranging from 0nM – 2nM. Table 2 shows the p-values by comparing all cell lines with each other for all the concentrations of NCS. As it can be seen from Fig 14 and Table 2, the mutant cell lines Art-/-, shTDP1 as wells as Art-/-.shTDP1 show marked sensitivity

to NCS as compared to WT cell line. Also, the sensitivity of the WT cells for NCS was significantly different from that of the mutant cells as WT cells showed higher survival percentage compared to the mutant cells. The sensitivity of the all the mutant cells was found to be remarkably the same at all concentrations of NCS. These results further validate the idea of an epistatic relationship between Artemis and TDP1.
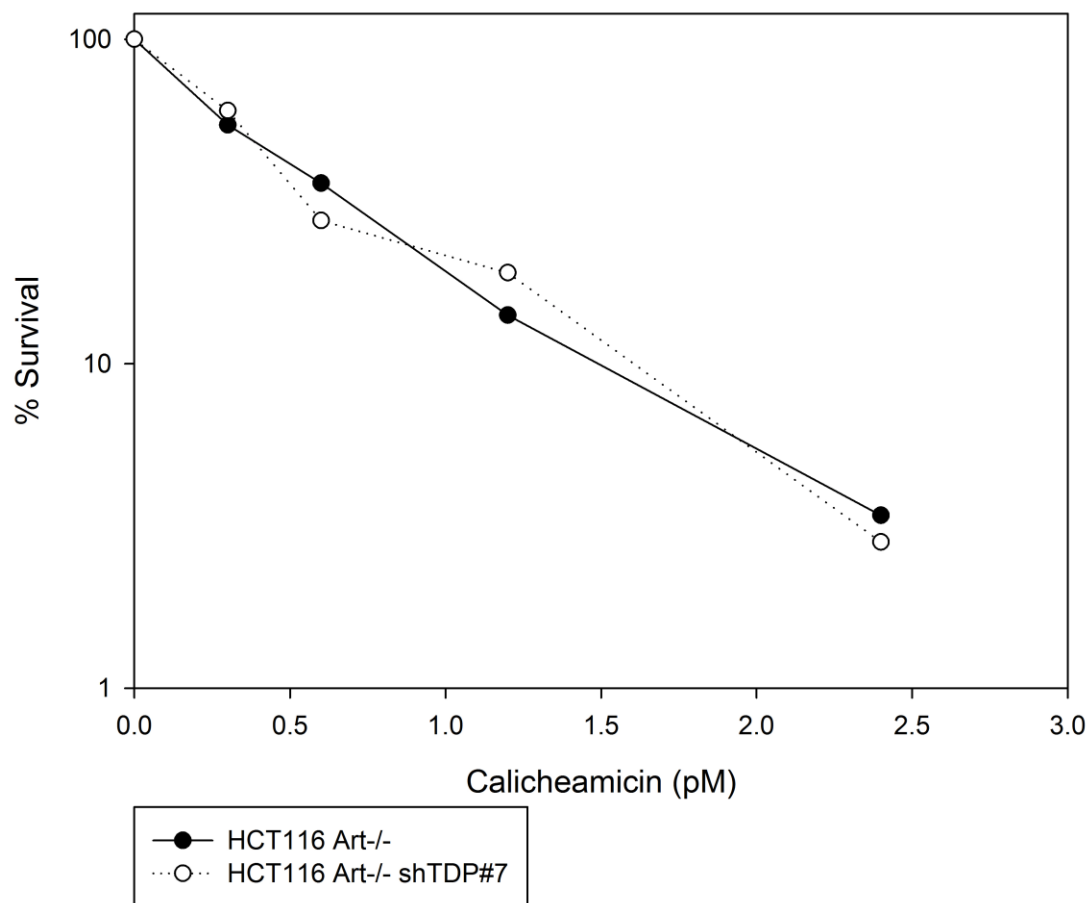
Figure 13 - Clonogenic Survival Assay with Calicheamicin

Artemis -/- and Artemis -/-.shTDP1 cell lines mentioned in the figure were seeded at different densities from 300/ dish to 10000/ dish in 60mm dishes. Following attachment, cells were treated with Calicheamicin within a concentration range of 0pM – 2.4pM for 6 hours. The drug was washed away and colonies were allowed to form for a period of 12 days. Colonies were later fixed with 100% methanol, stained with 0.5% Crystal Violet and colonies with minimum 50 cells were counted manually.
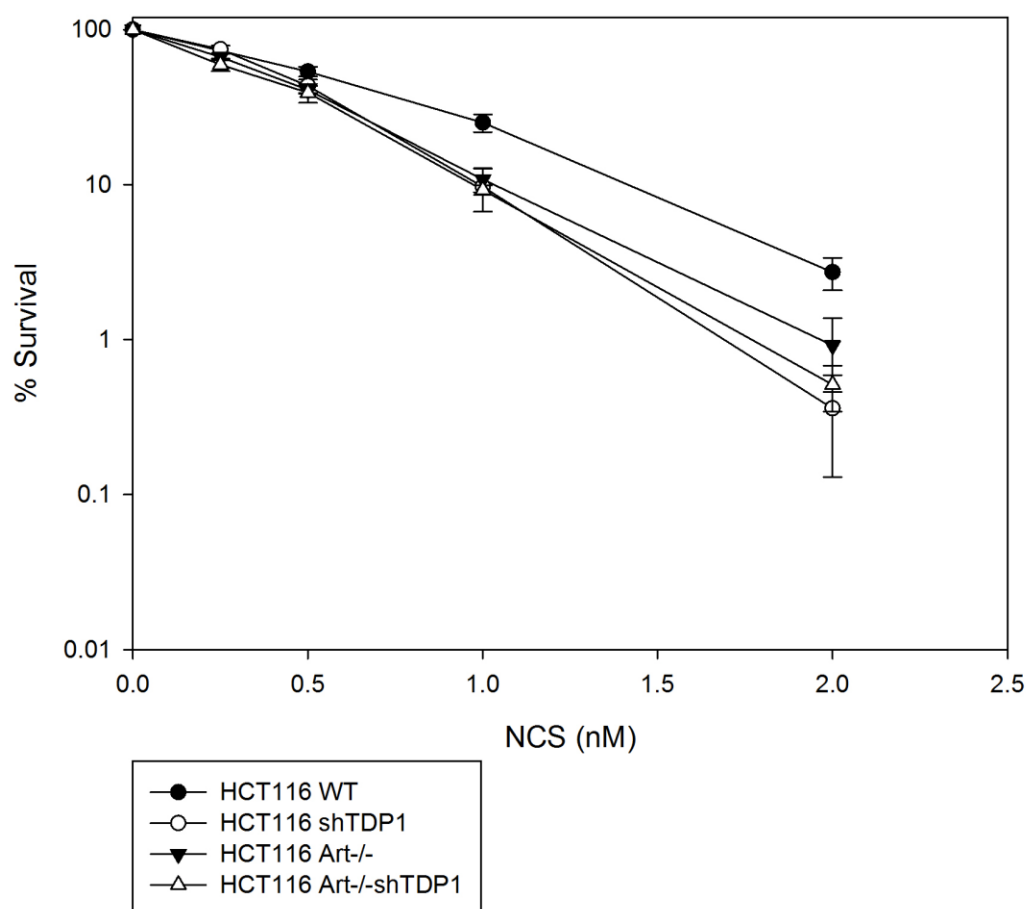
Figure 14 - Clonogenic Survival Assay with NCS

All the four cell lines mentioned in the figure were seeded at different densities from 300/ dish to 10000/ dish in 60mm dishes. Following attachment, cells were treated with NCS within a concentration range of 0nM – 2nM for 6 hours. The drug was washed away and colonies were allowed to form for a period of 12 days. Colonies were later fixed with 100% methanol, stained with 0.5% Crystal Violet and colonies with minimum 50 cells were counted manually. Error bars indicate S.E.M for 5 different experiments.

Table 2 - Significance Table

Table indicates p-values for all the four cell lines at all the different concentrations of NCS. Unpaired t-tests were carried out using GraphPad QuickCalcs software. Sensitivity of WT cells to NCS was found to be significantly different compared to all the mutant cell lines whereas the sensitivity of all the mutant cells to NCS showed no significant difference when compared with each other.

Cell Lines	P (0.25nM)	P (at 0.5nM)	P (at 1nM)	P (at 2nM)
WT vs shTDP1	-	0.11	0.0064	0.0067
WT vs Art-/-	-	0.02	0.0037	0.0483
WT vs Art-/-shTDP1	-	0.055	0.002	0.015
shTDP1 vs Art-/-	0.16	0.63	0.76	0.308
shTDP1 vs Art-/-shTDP1	0.056	0.558	0.89	0.627
Art-/- vs Art-/-shTDP1	0.257	0.766	0.48	0.47

3.5 Art-/- and Art-/-.shTDP1 cells show a similar increase in persistent 53BP1 foci:

In order to evaluate the role of Artemis and TDP1 in DSB repair, 53BP1 foci were quantified as a measure of residual DNA DSBs in all the four cell lines following NCS treatment. 53BP1 is a well-established and sensitive marker that relocates to multiple nuclear foci within minutes after exposure of cells to IR, co-localizes with known DNA damage response proteins like γ-H2AX and becomes hyperphosphorylated in response to IR (Ward, I. et al 2003) and radiomimetic drugs. It is general accepted that each 53BP1 focus represents an unrepaired DSB.

This 53BP1 Assay was performed using non-replicating G0/G1 cells to avoid spontaneous focus formation at stalled replication forks. The number of foci seen without drug treatment was similar in all the cell lines. The NCS treated samples showed a dramatic increase in the number of foci obtained and this increase was consistent with every cell line. As seen on Fig. 15 and 16, following 8 hours of repair, the WT cells showed a radical decrease in the number of foci as compared to the Art-/- and Art-/-.shTDP1 #7 cells. Thus there seems to be a clear repair defect in cells deficient in Artemis but deficiency of TDP1 in addition does not make the defect any more severe. Also, although the cells deficient in shTDP1 themselves may have a slight repair defect, it was not statistically significant.

HCT116 WT **HCT116 shTDP1**

Untreated

4nM NCS
(1 hour)

4nM NCS
(1 hour) +
8 hr
repair

HCT116 Art-/-   **HCT116 Art-/-.shTDP1#7**
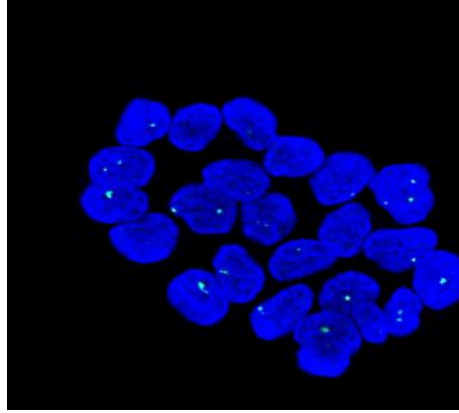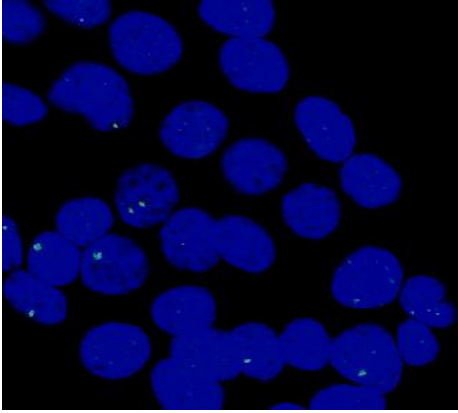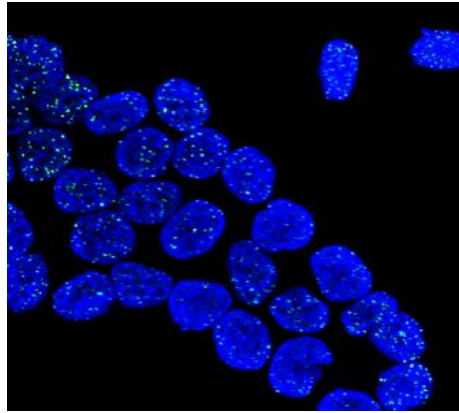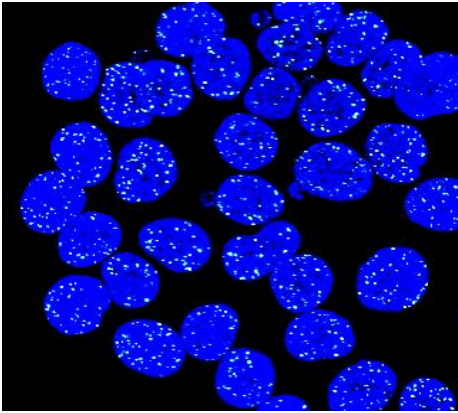
Untreated
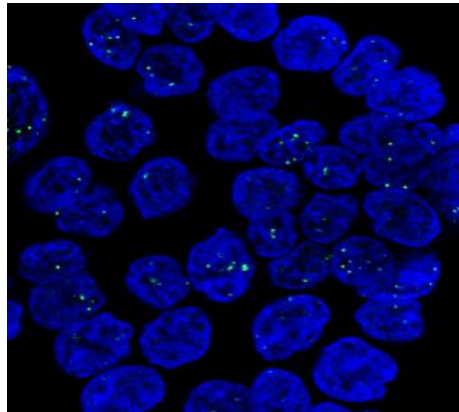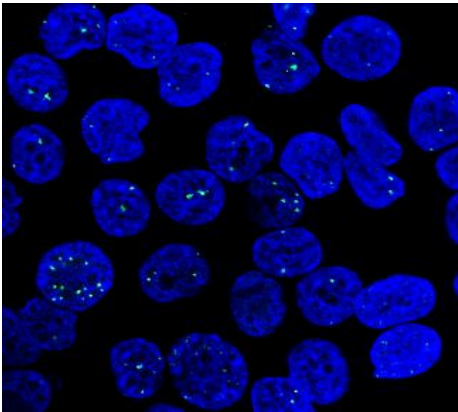
**4nM NCS
(1 hour)**

**4nM NCS
(1 hour) +
8 hr repair**
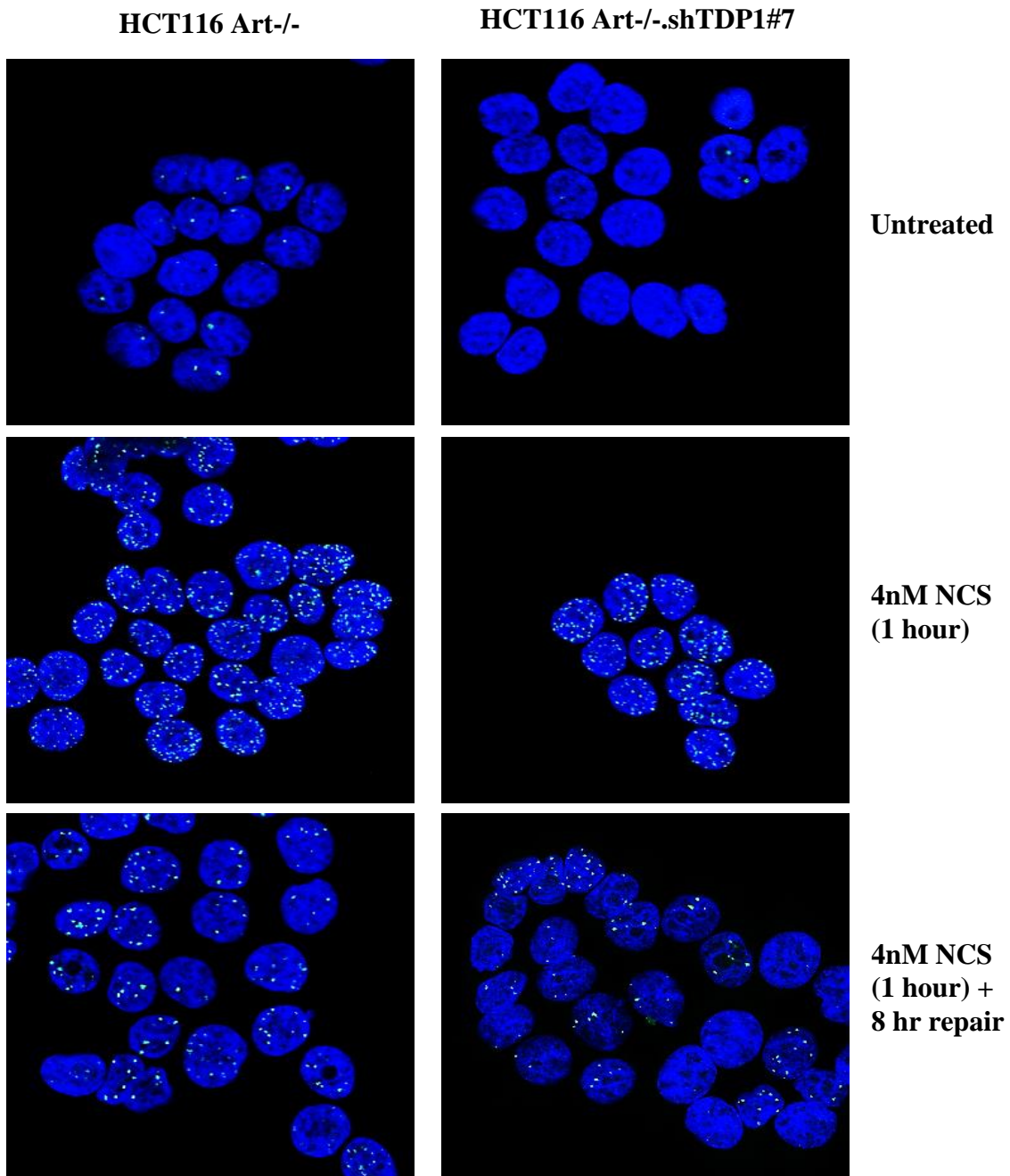
Figure 15 - Confocal images showing Nuclei (blue) and 53BP1 foci (green)

For the treated samples, 4nM NCS was added for 1 hour followed by processing of the cells either

immediately or following 8 hours of repair. Mouse Anti-53BP1 primary antibody diluted at 1:250

in casein blocker and Goat anti-mouse secondary antibody (Alexa Fluor 488) at 1:500 dilution

were used. Nuclei were counterstained with DAPI.
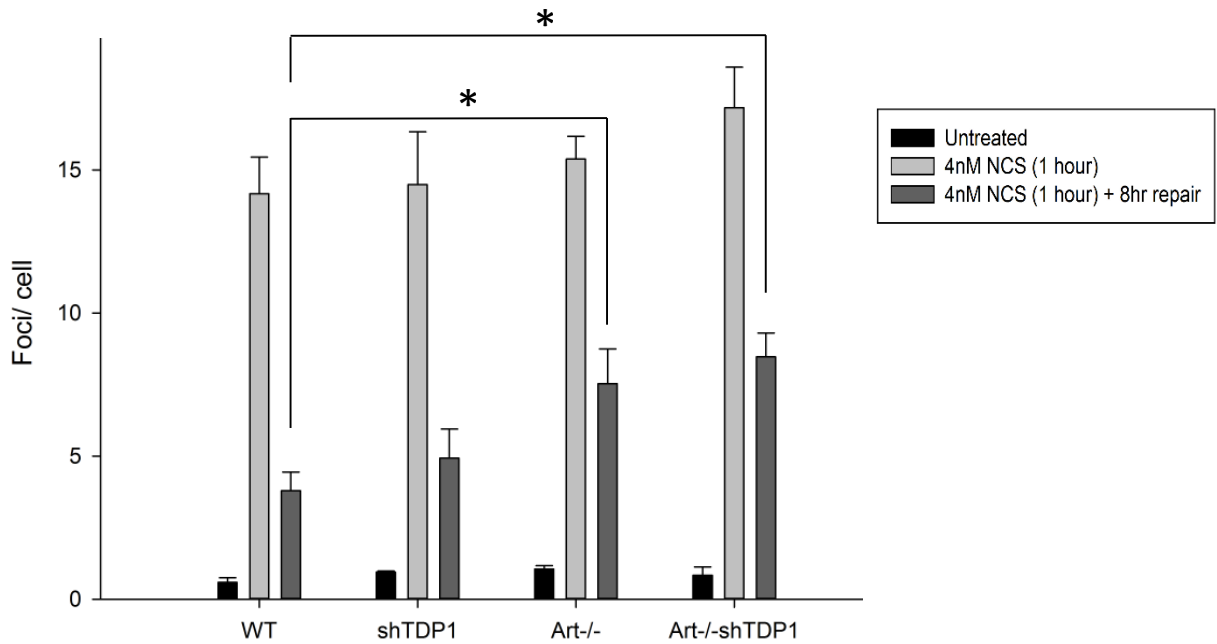
Figure 16 - Graphical Representation of 53BP1 focus formation assay

53BP1 focus assay was performed after 4nM NCS treatment. The panel displays number of foci formed per cell versus the different cell lines under different conditions. Error bars indicate S.E.M (n=3). After 8 hours of repair, p=0.03073 for WT vs Art-/- and p=0.006 for WT vs Art-/-.shTDP1#7.

Table 3 - Average number of Foci/ cell for different conditions

	Untreated	4nM NCS (1 hour)	4nM NCS (1 hour) + 8 hour repair
HCT116 WT	0.58	14.17	3.78
HCT116 shTDP1	0.94	14.48	4.92
HCT116 Art-/-	1.05	15.38	7.53
HCT116 Art-/-.shTDP1 #7	0.83	17.17	8.46

3.5 Deficiency of TDP1 enhances arrest in G1 phase in NCS-treated HCT116 cells.

TDP1 deficient cells showed a repair defect by 53BP1 that was not statistically significant. Since HCT116 are p53-proficient, they should show an ATM-meditated G1 block in response to DSBs. Therefore, if deficiency of TDP1 causes a DSB repair defect (due to less efficient PG removal) for NCS-induced DSBs, then the TDP1 deficient cells should show a greater G1 block from NCS than WT cells. In order to test this hypothesis, cell cycle analysis studies were performed.

An initial mapping experiment showing the basic cell cycle profiles of all the cell lines was carried out. All four cell lines were seeded at a density of 5×10^5 cells per 100mm dish. Cells were synchronised in G0/G1 phase of the cell cycle by culturing them in low serum medium (0.5% FBS) for 96 hours. As shown in Fig 17, around 65%-70% of the cell population was synchronised in G1 phase. Cells were released into serum and harvested at different time points in order to map their progression into S- and G2-phases. All cell lines were observed to progress in S-phase at around 12 hours after releasing into serum.

Once the progression of all the cell lines into S-phase was mapped, the cells were treated with 4nM NCS for 1 hour following serum starvation, released into serum and harvested at different time points. Fig 18 and 19 show the cell cycle profiles of all the four cell lines at different time points namely 24 hour control, 96 hour serum starved, and the 10, 12 and 14 hour release into serum with and without NCS treatment. Interestingly, as can be seen on Fig. 18 and 19, all the mutant cells showed a considerable lag in progression from G1- to S-phase after NCS treatment as compared to the WT cells. The enhanced G1 block in cells deficient in TDP1 at the 12 hour and the 14 hour time-points confirms the DSB repair defect in these cells. Artemis-deficient cells also show a similar enhanced G1 block in response to NCS treatment at the 12- and 14-hour time points. These

results demonstrate a similar epistasis between Artemis and TDP1 as seen with the clonogenic survival assay
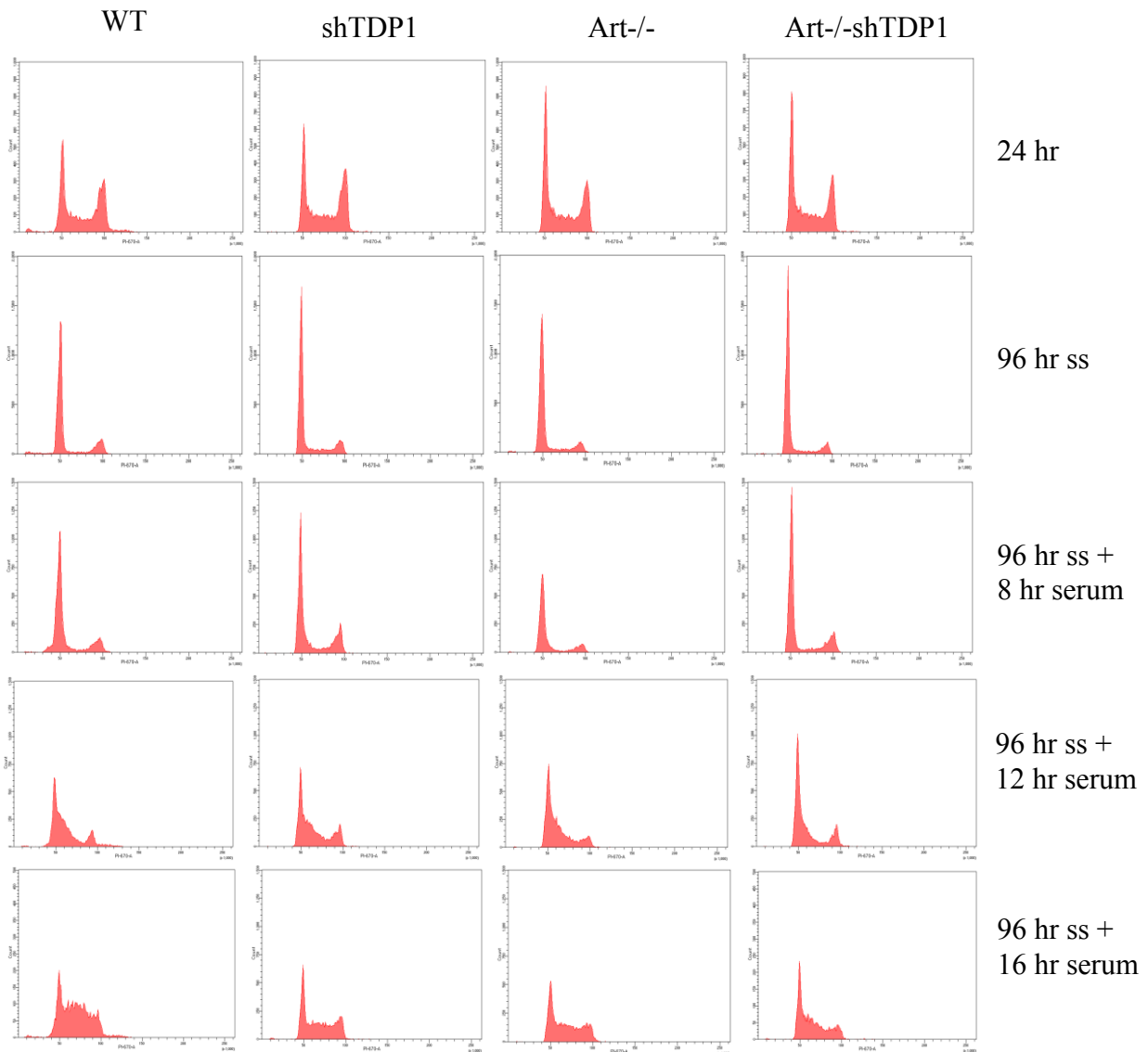
Figure 17 - Cell cycle analysis to map S-phase progression

Cells were serum starved for 96 hours, released serum and harvested at the time points mentioned above. All cell lines show a consistent profile with progression into S-phase observed at around 12 hours.
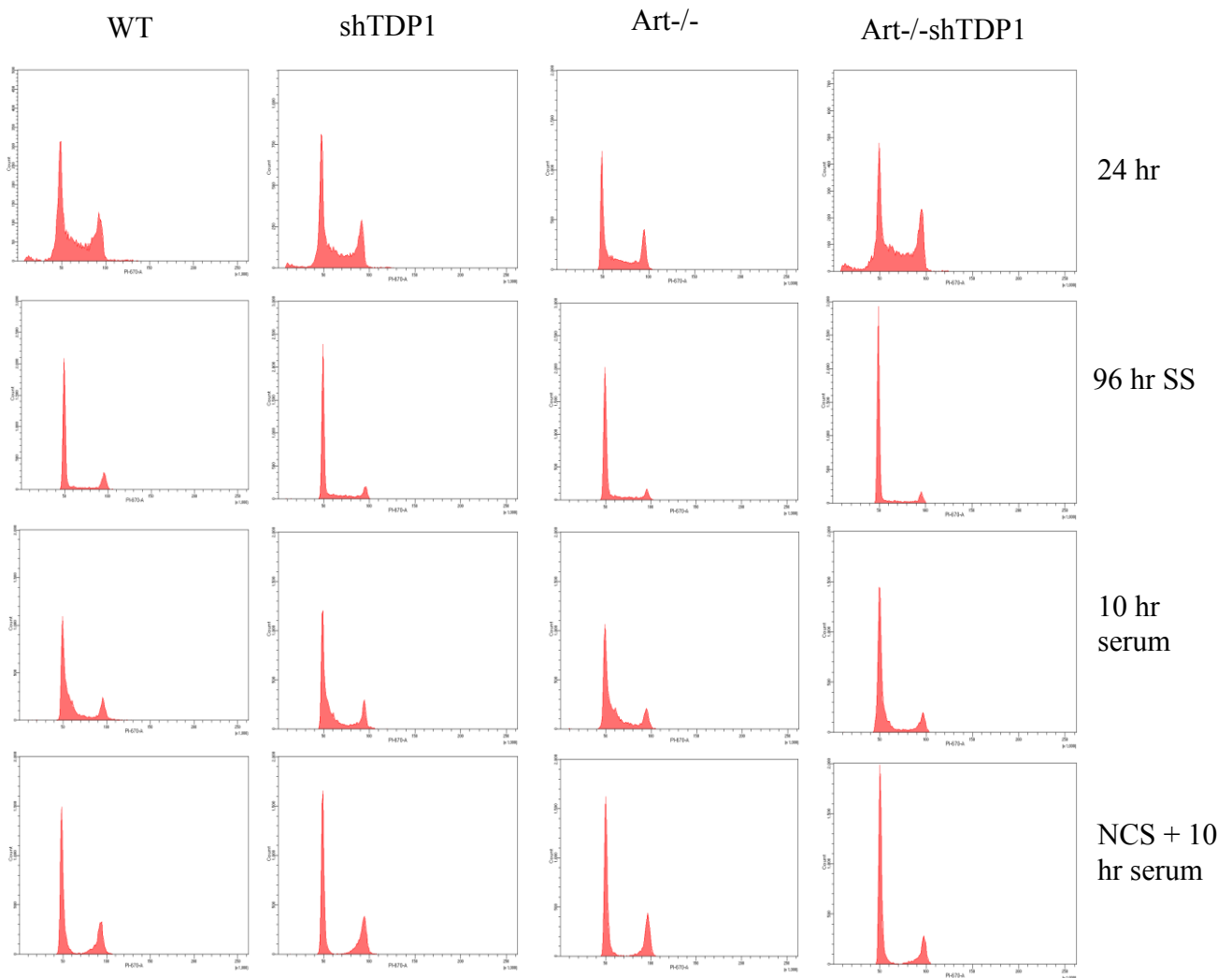
Figure 18 - Cell cycle analysis after NCS treatment for controls and 10 hour

5×10^5 cells were seeded in 100mm dishes and serum starved for 96 hours followed by the treatments mentioned in the figure. Analysis was performed on BD FACS calibre flow cytometer.
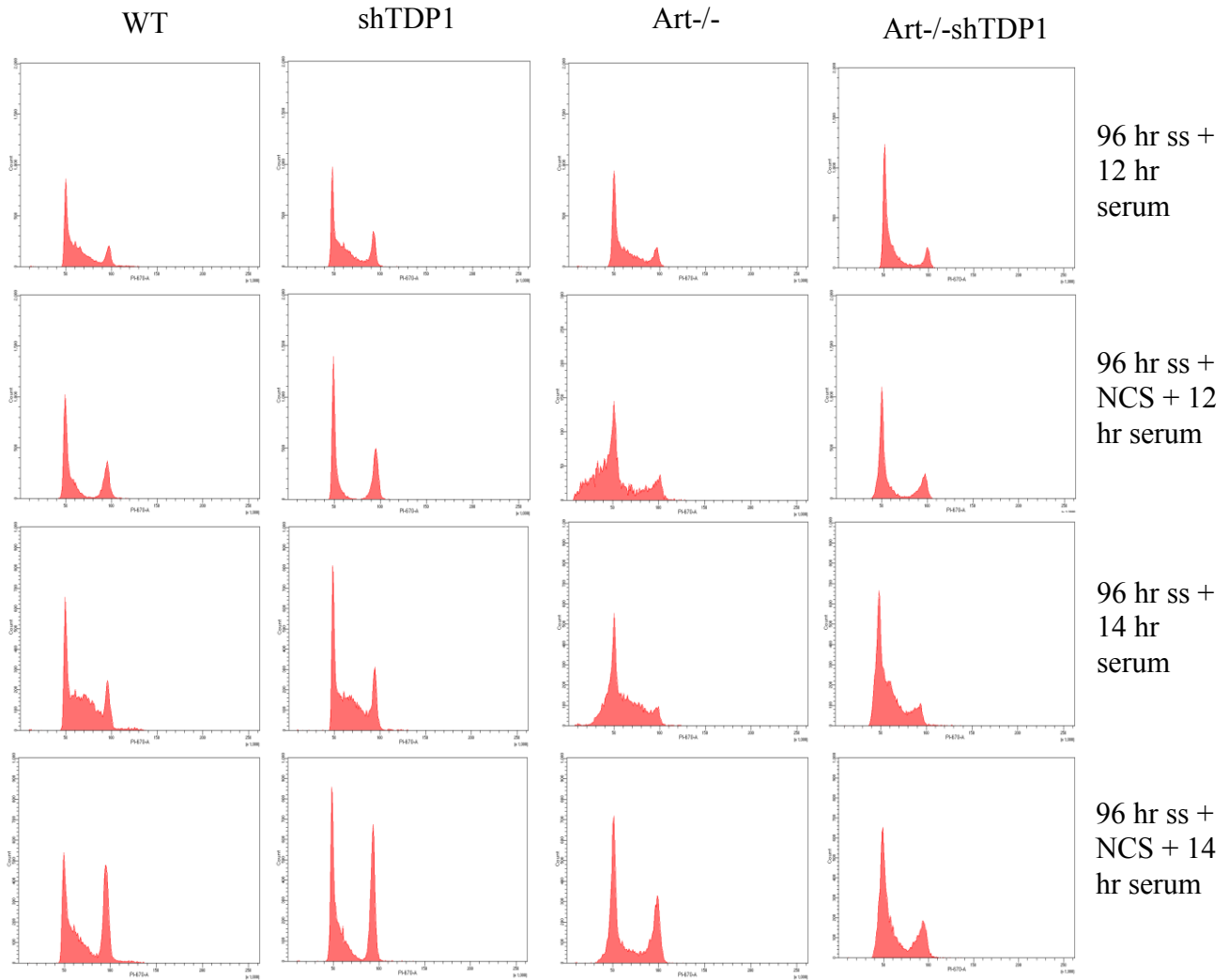
Figure 19 - Cell cycle Analysis following NCS treatment for 12 and 14 hours

5×10^5 cells were seeded in 100mm dishes and serum starved for 96 hours followed by the treatments mentioned in the figure. Analysis was performed on BD FACS calibre flow cytometer.

Table 4 – Percentage of Cell Population in G1, S and G2 phases

		G1-phase	S-phase	G2-phase
WT	24 hour control	34.1	40.3	25.5
	96 hour serum starved (ss)	66.1	16.5	17.4
	96 hr ss + NCS + 10 hr serum	57.3	16.3	26.4
	96 hr ss + NCS + 12 hr serum	40.1	29.4	30.5
	96 hr ss + NCS + 14 hr serum	19.3	45.9	34.8
shTDP1	24 hour control	36.1	40.2	23.7
	96 hour serum starved (ss)	65.7	23.9	10.3
	96 hr ss + NCS + 10 hr serum	57.9	14.1	27.9
	96 hr ss + NCS + 12 hr serum	48.1	15.1	36.8
	96 hr ss + NCS + 14 hr serum	27.4	33.3	39.3
Art-/-	24 hour control	34.8	43.4	21.8
	96 hour serum starved (ss)	67.7	21.5	10.9
	96 hr ss + NCS + 10 hr serum	58.5	10.6	30.8
	96 hr ss + NCS + 12 hr serum	41.4	18.8	39.8
	96 hr ss + NCS + 14 hr serum	48.2	19.8	31.9
Art-/-shTDP1	24 hour control	28.6	46.6	24.7
	96 hour serum starved (ss)	75.9	15.3	8.8
	96 hr ss + NCS + 10 hr serum	67.8	11.7	20.4
	96 hr ss + NCS + 12 hr serum	52.1	22.3	25.7
	96 hr ss + NCS + 14 hr serum	40.1	33.9	25.9

4. DISCUSSION, CONCLUSIONS AND FUTURE STUDIES

Potent cytotoxic DNA damaging agents have been the cornerstone of cancer treatment as few therapies have been successful against targets of growth signalling in cells (Rieder et al, 2011, Bianco et al, 2006, Anastas & Moon, 2012). Ionising radiation (Hutchinson, F. 1985), free radicals (Cadet et al, 2012) and radiomimetic drugs (Dedon & Goldberg, 1992) kill tumour cells by inducing double-strand breaks (DSBs) containing unligatable termini like 3′-phosphoglycolates (Zhou et al. 2005). The two different radiomimetic agents used in this thesis study viz. Calicheamicin and Neocarzinostatin, generate different types of 3′-PG terminated DNA double-strand breaks. NCS-induced DSBs have at one end a 5′-phosphate and a 3′-phosphate on a 2-base 3′-overhang. The opposite end has a 5′-aldehyde and either a 3′-PG or a 3′-phosphate on a one-base 3′-overhang (Povirk, 1996, Dedon & Goldberg, 1992). Calicheamicin produces an astonishingly high ratio of DSBs to SSBs with damaged products showing the presence of 3′-PG like residues and 5′-aldehyde-ended DNA fragments (Zein et al, 1988).

The sensitivity of tumour cells to these agents is strongly dependent on the efficiency of the repair of these DSBs by the tumour cells. Non-Homologous End Joining (NHEJ) is the pathway of choice

by which the DSBs are repaired, apart from Homologous Recombination Repair (HRR), and is prevalent throughout the cell cycle, predominantly in G1 phase (Guirouilh-Barbat et al., 2004). The end groups produced as a result of NCS or Calicheamicin treatment can block the activity of various DNA repair proteins including DNA Ligase IV and DNA Polymerases. Thus, in order to efficiently repair damage, it is essential that these end lesions be removed. Artemis and TDP1 are such end-processing enzymes involved in the repair of DSBs.

Artemis was originally identified as the gene which codes for a V(D)J recombination/ DNA repair factor belonging to the metallo-β-lactamase family of proteins. It was later found out that Artemis is the principal nuclease involved in NHEJ which predominantly resolves these unligatable termini, especially the 3′ blocks, by nucleolytic trimming in order to obtain juxtaposable ends that can be annealed and finally ligated (Povirk, 2013). Artemis-null cells displayed increased sensitivity to a potent Top II inhibitor, etoposide (Kurosawa et al., 2008). It is known that DNA Ligase IV is able to ligate incompatible DNA ends containing 3′ overhangs of 2-4 bases (Ma et al, 2002) and thus it was believed that Artemis plays a role in NHEJ only when the ends have to be processed before ligation. Some studies have suggested an epistatic interaction of Artemis with ATM in promoting radiosurvival and DSB repair, even in growth-arrested cells which ideally would not be subject to effects with respect to changes in cell cycle.

Tyrosyl-DNA phosphodiesterase 1 (TDP1) is an enzyme which removes the peptide fragments linked through tyrosine to the 3′ end of DNA in these Topoisomerase 1-mediated breaks (Das et al., 2009). A hereditary homozygous mutation at the active site of TDP1 has been shown to be the cause of Spinocerebellar Ataxia with Axonal Neuropathy (SCAN1) (Takashima et al. 2002). TDP1 is also known to be involved in 3′-phosphoglycolate processing. Previous studies from the lab have shown that whole-cell extracts from SCAN1 cells have a deficiency in processing of protruding 3′-phosphoglycolate termini to 3′-phosphates, both on single-strand

as well as double-strand breaks (Zhou et al. 2005). This deficiency of the mutant TDP1 in SCAN1 cells compared to the wild type TDP1 is attributed to the long half-life of mutant TDP1 covalently linked to DNA as compared to the Wild-type which has infinitesimally short half-life (Das et al., 2009).

This thesis investigates whether TDP1 and Artemis are alternative end-processing enzymes in NHEJ and if they reveal any epistasis with each other in response to NCS-mediated DNA double-strand breaks containing modified 3′-phosphoglycolate ends. Both shRNA-mediated knockdown of TDP1 and knockout of Artemis result in sensitivity to Neocarzinostatin (NCS) and Calicheamicin, radiomimetic drugs that produce 3′-phosphoglycolate terminated double-strand breaks. In that effect, we produced a cell line with combined deficiency in Artemis and TDP1. To generate such a cell line, Art-/- HCT116 colon carcinoma cells were infected with a Lentivirus expressing a TDP1 shRNA. Clones were selected in puromycin, and screened for stable integration of the puromycin N-acetyltransferase (pac) gene. Positive clones were screened for maximum TDP1 knockdown which was found to be around 12 times.

We wanted to examine the phenotypic implications of the deficiency of these two repair proteins in HCT116 cell line. Several studies have shown that cells lacking important DNA repair proteins grow slower as compared to their proficient counterparts (Frank et al., 2000, Van Nguyen et al, 2007). Cells deficient in Ligase IV, the principal ligase involved in NHEJ, and Rad54, an HR protein, individually experienced growth cessation relative to wild type control cells. Double deficient RL cells (Rad54-/- and LigIV-/-) were even more severely compromised for growth (Mills, 2004). In order to observe if this effect extends to our study, we performed a growth curve experiment in order to observe if deficiency of Artemis and TDP1 cause the cells to grow slower. Our results indicated that the double mutants had a marked growth retardation phenotype as compared to the cells proficient in these proteins thus coinciding with the previous studies. Cells have evolved cell cycle checkpoints in order to

prevent the daughter cells from receiving a damaged copy of the genome from the parent cell. Activation of specific checkpoints causes the cells to arrest in those specific phases of the cell cycle, repair the damage inflicted on the genome followed by resumption of the cell cycle allowing the cell to progress through the phases and ultimately divide. This could be an interesting hypothesis for the slower growth rate of the cells as these repair deficient cells would activate the checkpoints in order to prevent the damage from passing on to the next generation of cells.

Epistasis studies have helped scientists to elucidate whether two proteins are functional in a particular DNA repair pathway (Glassner & Mortimer, 1994, Symington, 2002, Jensen et al, 2013). If deficiency of one protein renders the cells sensitive to particular DNA damaging agents, however, eliminating another protein from these cells does not further sensitize them to the treatment, it would implicate the presence of these two proteins in the same pathway, albeit performing different roles in it (Ishii & Inoue, 1989). On the other hand, if the two proteins have similar functional roles, then in cells subjected to DNA damage, deficiency of both the proteins would be synthetically lethal meaning the cells would demonstrate a higher sensitivity as compared to the single mutant cells.

We carried out clonogenic survival assays on these derivative HCT116 cell lines namely wild type, shTDP1, Art-/- and Art-/-.shTDP1 to see if Artemis and TDP1 are alternative end trimming enzymes or they are involved in the same pathway. The result was extremely surprising as these experiments demonstrate that Artemis and TDP1 are epistatic in their function in promoting cell survival following induction of NCS- and Calicheamicin-mediated double-strand breaks. In other words, the sensitivity of Artemis or TDP1 deficient cells to these agents was no less than the sensitivity of the cells having a combined deficiency of Artemis and TDP1. Immunofluorescence studies were also performed on these derivative cell lines to check for the ability of the cells to repair NCS-mediated DSBs. 53BP1 is one of the earliest

signalling molecules to get activated following DNA damage and is recruited to the site of the damage (Panier & Boulton, 2013). By tracing the accumulation of 53BP1 protein at the site of chromatin damage as sub-nuclear foci using a Confocal Microscope at different time points, one can assess the ability of the cells in repair of the damaged chromatin. This study has shown a similar increase in persistent 53BP1 foci in the Art-/- and the double mutant Art-/-.shTDP1 #7 cell lines thus proving the point above that shTDP1 does not make the deficiency any more severe. It was interesting to note that the size of a focus was small immediately after NCS treatment but then increased during the repair period. As the cell encounters damage, a large number of proteins get dispersed throughout the genome at the damaged areas thus reducing the size of an individual focus. Following repair, these proteins would either be degraded by ubiquitination or migrate to other unrepaired areas in the genome.

The epistatic relationship between Artemis and TDP1 could also implicate these two proteins performing secondary roles in the NHEJ pathway apart from their primary function which is end-processing. Indeed, recently a group has revealed novel interesting associations of TDP1 with core NHEJ proteins. TDP1 interacts and binds directly to XLF and Ku 70/80 (Heo et al., 2015). TDP1 also promoted DNA binding by Ku and XLF apart from participating in multiprotein-DNA complexes with XLF and Ku70/80. As Ku 70/80 and XLF are known to be some of the earliest proteins recruited to the double-strand break site, TDP1 is also suggested to be recruited in the early stages of NHEJ even prior to DNA-PKcs. The obstacle of DNA-PKcs blocking the ends preventing premature access to end-processing enzymes would be bypassed by this early recruitment of TDP1 at the break site which can then carry out its function of resolving exposed 3′-ends to generate 3′-phosphates (Heo et al., 2015).

DNA Ligase IV is a part of the Ligase IV complex in NHEJ containing XRCC4/XLF/Ligase IV which is absolutely required for end-joining. Several studies have found that Ligase IV deficient cells were extremely sensitive to ionizing radiation (Grawunder et al, 1998). DT40

Chicken lymphocytes lacking Ligase IV (LigIV-/-) showed marked sensitivity to X-rays and bleomycin (Adachi, et al 2001). Ligase IV and TDP1 cells show severe growth retardation as compared to the WT, TDP1 deficient and even Artemis and TDP1 double deficient cells. In the future, we wish to answer the question whether the sensitivity of TDP1 is due to impaired NHEJ by performing a clonogenic survival assay with cells double deficient in Ligase IV and TDP1.

Poly (ADP-ribose) Polymerases are recruited to the DNA damage sites and attach poly (ADP-ribose) (PAR) chains to various proteins including themselves and chromatin (Guillot et al., 2014). In fact, PARP1-deficient cells were highly sensitive to camptothecin, an anti-cancer drug that trap Top1 cleavage complexes (Das et al., 2014). PARP and TDP1 have been shown to be epistatic for the repair of the Top1 cleavage complexes and that TDP1 PARylation enhances its recruitment to DNA damage sites without interfering with TDP1 catalytic activity (Das et al., 2014). We would, in the future, seek to explore this possibility of involvement of PARP1 in repair of NCS/ Calicheamicin-mediate lesions by TDP1 by the action of Olaparib, a PARP1 inhibitor (Murai et al, 2014).

Another surprising observation was the statistically insignificant repair deficiency in the shTDP1 cells in the 53BP1 focus assay, as compared to the significant difference in their survival ability in the clonogenic survival assays in response to DNA damage by NCS. This behaviour of cells could be explained by the hypothesis that the survival assays were carried out on unsynchronised cells. TDP1 lethality in S-phase is attributed to the accumulation of unresolved Top1 cleavage complexes during DNA replication. When a replication fork is progressing towards these stalled Top1 cc, the extension of the leading strand is terminated with replication fork run-off resulting in the conversion of the SSBs into DSBs following a round of DNA replication (Tsao et al, 1993, Strumberg, et al. 2000). In addition, when cells are treated with a DNA damaging agent like NCS, an exponential increase in strand breaks

would further enhance the sensitivity of the cells thus attributing to the phenotype observed in the clonogenic survival assays. The 53BP1 assay, on the other hand, was performed on serum-starved cells synchronised in G1 phase. This would almost eliminate the formation of DSBs from Top1 cleavage complexes or from NCS-induced single-strand breaks in these cells and thus the deficiency is attributed entirely to the DSBs formed as a result of NCS treatment. In this case, Artemis would be sufficient to process the ends formed as a result of the NCS-mediated damage and thus this would explain the slight, but statistically insignificant, repair deficiency observed in the 53BP1 Assay.

TDP1, as mentioned above, has been known to play a major role in resolution of Top1 mediated breaks during replication. Replication forks can collide with single-strand breaks leading to the formation of potentially hazardous double-strand breaks. As the 53BP1 assay showed insignificant repair deficiency in the TDP1 knockdown cells when they were synchronised in the G1 phase, we would like to investigate whether the sensitivity of shTDP1 mutant cells is replication dependent. In other words, does deficiency of TDP1 prevent the repair of Top1-mediated SSBs which could be later converted to harmful DSBs? Aphidicolin is DNA replication inhibitor, which primarily acts on DNA polymerase Alpha while also competing with dCTP incorporation (Krokan, Wist & Krokan, 1981). Inhibiting replication will prevent the conversion of SSBs to DSBs and thus shTDP1 cells should be no less sensitive than those cells containing functional TDP1. Consequently, a result similar to the 53BP1 assay would be expected.

Several studies have associated TDP1 with DNA damage response. It was observed that ATM and DNA-PK both can regulate TDP1 through phosphorylation of serine 81 in response to DSBs associated with the trapping of Top1-DNA complexes and IR. Cells deficient in TDP1 or harbouring a TDP1[S81A] phosphomutant show enhanced formation of DSBs. (Das, B. et al 2009). However, no group has till yet studied the function of TDP1 in cell cycle progression in

HCT116 cells. The role of Artemis in cell cycle progression is well studied as groups have come up with contrasting conclusions. Jeggo and colleagues have shown that cells deficient in Artemis exhibit a prolonged G2/M arrest following IR irradiation (Kurosawa & Adachi, 2010) while Legerski and group have presented data showing that Artemis was required for G2/M arrest as knockdown of Artemis resulted in an accelerated release from the IR-induced G2/M checkpoint (Geng et al, 2007). In order to further understand the phenotypic implications of Artemis and TDP1 deficient cells on cell cycle progression, we performed cell cycle profile analysis studies on all the four cell lines in response to NCS-mediated DNA DSB formation. A mapping experiment performed initially gave an indication of the time the cells require to progress through the cell cycle. All the cell lines showed a consistent G1/S progression without NCS treatment. However, on treating the cells with NCS, TDP1-deficient cells show a substantial retardation in the progression from G1 to S-phase. This phenotype could be attributed to the fact that TDP1 is an early NHEJ protein interacting with Ku 70/80 and XLF apart from carrying out end-processing functions. NCS-treated cells suffer damage in the form of DSBs, which have to be repaired prior to entry into S-phase. In that case, TDP1 deficiency would prevent the cells from exiting the G1 phase as inefficient NHEJ would allow residual damage to persist which, only once repaired, would allow the cells progress into S-phase.

Another interesting observation was the extensive decrease in the cell population of the double mutants in the G2 phase as compared to all the other cell lines. This behaviour could be explained with keeping the end-processing roles of Artemis and TDP1 in mind. Artemis is a known NHEJ end-trimming nuclease while several studies have implicated the role of TDP1 in NHEJ as an end-processing enzyme. TDP1 deficiency is also lethal in S-phase as the unresolved Top1cc accumulate. In that case, deficiency of Artemis and TDP1, would thus prevent cells from entering the G2 phase. Another hypothetical reason behind this decrease in the G2 cell population could be assigned to the cycling of the cells from the G2 phase back into

G1. These cells that have escaped the checkpoints in the initial cell cycle would accumulate excessive damage and after cycling back into the G1 phase, would accumulate there, thus decreasing the population of cells in G2. This theory can be examined by performing cell cycle experiments with the addition of Nocodazole which would prevent the cells from cycling back into G1 (Rosner, Schipany & Hengstschläger, 2013).

In conclusion, we have observed that TDP1 and Artemis do not exhibit synthetic lethality but manifest and epistatic relationship with each other. Numerous small 53BP1 foci were formed corresponding to DSBs following NCS treatment. As the cell repairs the damage, the foci become less numerous but some are still visible after 8 hours of repair and increase in size during that time, suggesting that repair proteins continue to accumulate at the sites of persistent DSBs. As observed from the cell cycle studies, enhanced G1 block in response to NCS in shTDP1 cells suggests that TDP1 is an important protein for DSB repair, presumably by NHEJ, in the G1 phase of the cell cycle, deficiency of which causes the cells to arrest in G1 phase.

REFERENCES

1. Adachi N, Ishino T, Ishii Y, Takeda S, Koyama H (2001) DNA ligase IV-deficient cells are more resistant to ionizing radiation in the absence of Ku70: Implications for DNA double-strand break repair. Proc Natl Acad Sci U S A 98: 12109–12113

2. Akopiants, K., Mohapatra, S., Menon, V., Zhou, T., Valerie, K., & Povirk, L. (2014). Tracking the processing of damaged DNA double-strand break ends by ligation-mediated PCR: Increased persistence of 3'-phosphoglycolate termini in SCAN1 cells. *Nucleic Acids Research,* 3125-3137.

3. Anastas, J., & Moon, R. (2012). WNT signalling pathways as therapeutic targets in cancer. Nat Rev Cancer, 13(1), 11-26. doi:10.1038/nrc3419

4. Bayer, R. A., Gaynor, E. R. & Fisher, R. I. (1992). Bleomycin in Non-Hodgkin's lymphoma. *Semin. Oncol.* 19, 46–52

5. Bianco, R., Melisi, D., Ciardiello, F., & Tortora, G. (2006). Key cancer cell signal transduction pathways as therapeutic targets. European Journal Of Cancer, 42(3), 290-294. doi:10.1016/j.ejca.2005.07.034

6. Branzei, D. and M. Foiani, 2007. Template Switching: From Replication Fork Repair to Genome Rearrangements. *Cell*, 131 (7): 1228-1230

7. Budanov, A. (2004). Regeneration of Peroxiredoxins by p53-Regulated Sestrins, Homologs of Bacterial AhpD. *Science,* 596-600

8. Bunting, S., & Nussenzweig, A. (2013). End-joining, translocations and cancer. Nat Rev Cancer, 13(7), 443-454. doi:10.1038/nrc3537

9. Cadet, J., Ravanat, J., TavernaPorro, M., Menoni, H., & Angelov, D. (2012). Oxidatively generated complex DNA damage: Tandem and clustered lesions. Cancer Letters, 327(1-2), 5-15. doi:10.1016/j.canlet.2012.04.005

10. Chaudhry, M., Dedon, P., Wilson, D., Demple, B., & Weinfeld, M. (1999). Removal by Human Apurinic/Apyrimidinic Endonuclease 1 (Ape 1) and Escherichia coli Exonuclease III of 39-Phosphoglycolates from DNA Treated with Neocarzinostatin, Calicheamicin, and gamma radiation. *Biochemical Pharmacology, 57*, 531-538.

11. Chen, J., & Stubbe, J. (2005). BLEOMYCINS: TOWARDS BETTER THERAPEUTICS. *Nature Reviews Cancer, 5*, 102-112.

12. Das, B., Antony, S., Gupta, S., Dexheimer, T., Redon, C., & Garfield, S., Pommier, Y. (2009). Optimal function of the DNA repair enzyme TDP1 requires its phosphorylation by ATM and/or DNA-PK. The EMBO Journal, 28(23), 3667-3680. doi:10.1038/emboj.2009.302

13. Das, B., Huang, S., Murai, J., Rehman, I., Ame, J., & Sengupta, S. et al. (2014). PARP1-TDP1 coupling for the repair of topoisomerase I-induced DNA damage. Nucleic Acids Research, 42(7), 4435-4449. doi:10.1093/nar/gku088.

14. Dasgupta, D., and Goldberg, I. H. (1985). Mode of reversible binding of neocarzinostatin chromophore to DNA evidence for binding via the minor groove. *Biochemistry,* 24, 6913-6920.

15. Davies, D., Interthal, H., Champoux, J., & Hol, W. (2002). The Crystal Structure of Human Tyrosyl-DNA Phosphodiesterase, Tdp1. *Structure, 10*, 237-248.

16. Davis, A., & Chen, D. (2013). DNA double-strand break repair via non-homologous end-joining. *Transl Cancer Res, 2*(3), 130-143.

17. De Bont, R. and N. van Larebeke, 2004. Endogenous DNA damage in humans: a review of quantitative data. *Mutagenesis*, 19 (3): 169-185.

18. Debéthune, L., Kohlhagen, G., Grandas, A., & Pommier, Y. (2002). Processing of nucleopeptides mimicking the topoisomerase I–DNA covalent complex by tyrosyl-DNA phosphodiesterase. *Nucleic Acids Research, 30*(5), 1198-1204.

19. Dedon, P., & Goldberg, I. (1992). Free-Radical Mechanisms Involved in the Formation of Sequence-Dependent Bistranded DNA Lesions by the Antitumor Antibiotics Bleomycin, Neocarzinostatin, and Calicheamicin. *Chemical Research in Toxicology, 5*(3), 311-332.

20. Einhorn, L. H. (2002). Curing metastatic testicular cancer. *Proc. Natl Acad. Sci.* USA 99, 4592–4595

21. Frank, K., Sharpless, N., Gao, Y., Sekiguchi, J., Ferguson, D., & Zhu, C. et al. (2000). DNA Ligase IV Deficiency in Mice Leads to Defective Neurogenesis and Embryonic Lethality via the p53 Pathway. *Molecular Cell*, *5*(6), 993-1002. doi:10.1016/s1097-2765(00)80264-6

22. Geng L, *et al* (2007) Artemis links ATM to G2/M checkpoint recovery via regulation of Cdk1-cyclin B. *Mol Cell Biol* **27**: 2625–2635.

23. Geng, L., Zhang, X., Zheng, S., & Legerski, R. (2007). Artemis Links ATM to G2/M Checkpoint Recovery via Regulation of Cdk1-Cyclin B. Molecular And Cellular Biology, 27(7), 2625-2635. doi:10.1128/mcb.02072-06

24. Glassner, B., & Mortimer, R. (1994). Synergistic Interactions between RAD5, RAD16 and RAD54, Three Partially Homologous Yeast DNA Repair Genes Each in a Different Repair Pathway. Radiation Research, 139(1), 24. doi:10.2307/3578728

25. Goodarzi, A., Yu, Y., Riballo, E., Douglas, P., Walker, S., & Ye, R. et al. (2006). DNA-PK autophosphorylation facilitates Artemis endonuclease activity. The EMBO Journal, 25(16), 3880-3889. doi:10.1038/sj.emboj.7601255

26. Grawunder, U., Zimmer, D., Fugmann, S., Schwarz, K., & Lieber, M. (1998). DNA Ligase IV Is Essential for V(D)J Recombination and DNA Double-Strand Break Repair in Human Precursor Lymphocytes. Molecular Cell, 2(4), 477-484. doi:10.1016/s1097-2765(00)80147-1

27. Guillot, C., Favaudon, V., Herceg, Z., Sagne, C., Sauvaigo, S., & Merle, P. et al. (2014). PARP inhibition and the radiosensitizing effects of the PARP inhibitor ABT-888 in in vitro hepatocellular carcinoma models. BMC Cancer, 14(1), 603. doi:10.1186/1471-2407-14-603

28. Guirouilh-Barbat, J., Huck, S., Bertrand, P., Pirzio, L., Desmaze, C., Sabatier, L., & Lopez, B. (2004). Impact of the KU80 Pathway on NHEJ-Induced Genome Rearrangements in Mammalian Cells. Molecular Cell, 14(5), 611-623. doi:10.1016/j.molcel.2004.05.008

29. Han, W., & Yu, K. (2010). Ionizing Radiation, DNA Double-strand Break and Mutation. *Advances in Genetic Research* (Vol. 4). Nova Science.

30. Heo, J., Li, J., Summerlin, M., Hays, A., Katyal, S., & McKinnon, P. et al. (2015). TDP1 promotes assembly of non-homologous end joining protein complexes on DNA. DNA Repair, 30, 28-37. doi:10.1016/j.dnarep.2015.03.003

31. Hutchinson, F., (1985). Chemical changes induced in DNA by ionizing radiation. *Progress in Nucleic Acid Research and Molecular Biology, 32*, 115-154.

32. Interthal, H., Pouliot, J., & Champoux, J. (2001). The tyrosyl-DNA phosphodiesterase Tdp1 is a member of the phospholipase D superfamily. *PNAS, 98*(21), 12009-12014.

33. Ishii, C., & Inoue, H. (1989). Epistasis, photoreactivation and mutagen sensitivity of DNA repair mutants upr-1 and mus-26 in Neurospora crassa. Mutation Research/DNA Repair, 218(2), 95-103. doi:10.1016/0921-8777(89)90015-3

34. Jensen, R., Ozes, A., Kim, T., Estep, A., & Kowalczykowski, S. (2013). BRCA2 is epistatic to the RAD51 paralogs in response to DNA damage. DNA Repair, 12(4), 306-311. doi:10.1016/j.dnarep.2012.12.007

35. Kappen. L.S., I.H. Goldberg and J.M. Liesch. (1982). Identification of thymidine-5′ - aldehyde at DNA strand breaks induced by neocarzinostatin chromophore. *Proc. Natl. Acad. Sci*. USA. 79. 744-748.

36. Krokan, H., Wist, E., & Krokan, R. (1981). Aphidicolin inhibits DNA synthesis by DNA polymerase α and isolated nuclei by a similar mechanism. Nucl Acids Res, 9(18), 4709-4719. doi:10.1093/nar/9.18.4709

37. KUROSAWA, A., & ADACHI, N. (2010). Functions and Regulation of Artemis: A Goddess in the Maintenance of Genome Integrity. JRR, 51(5), 503-509. doi:10.1269/jrr.10017

38. Kurosawa, A., Koyama, H., Takayama, S., Miki, K., Ayusawa, D., & Fujii, M. et al. (2008). The Requirement of Artemis in Double-Strand Break Repair Depends on the Type of DNA Damage. DNA And Cell Biology, 27(1), 55-61. doi:10.1089/dna.2007.0649

39. Langer, J.A., A.S. Acharya and P.B. Moore, 1975. Characterization of the particles produced by exposure of ribosomal subunits to urea. *Biochim. Biophys. Acta*, 407 (3): 320-324.

40. Lee, M., Ellestad, G., & Borders, D. (1991). Calicheamicins: Discovery, Structure, Chemistry, and Interaction with DNA. *Acc. Chem. Res, 24*, 235-243.

41. Lees-Miller, S., & Meek, K. (2003). Repair of DNA double-strand breaks by non-homologous end joining. *Biochimie, 85*, 1161-1173.

42. Li, L., Drayna, D., Hu, D., Hayward, A., Gahagan, S., Pabst, H., & Cowan, M. (1998). The Gene for Severe Combined Immunodeficiency Disease in Athabascan-Speaking Native Americans Is Located on Chromosome 10p. The American Journal Of Human Genetics, 62(1), 136-144. doi:10.1086/301688

43. Li, L., Moshous, D., Zhou, Y., Wang, J., Xie, G., & Salido, E. et al. (2002). A Founder Mutation in Artemis, an SNM1-Like Protein, Causes SCID in Athabascan-Speaking Native Americans. The Journal Of Immunology, 168(12), 6323-6329. doi:10.4049/jimmunol.168.12.6323

44. Lieber, M., Ma, Y., Pannicke, U., & Schwarz, K. (2003). Mechanism and Regulation of Human Non-Homologous End-Joining. *Nature Reviews Molecular Cell Biology, 4*, 712-720.

45. Ma, Y., Pannicke, U., Schwarz, K., & Lieber, M. (2002). Hairpin Opening and Overhang Processing by an Artemis/DNA-Dependent Protein Kinase Complex in Non-homologous End Joining and V(D)J Recombination. Cell, 108(6), 781-794. doi:10.1016/s0092-8674(02)00671-2

46. Mahajan, K., S. Nick McElhinny, B. Mitchell and D. Ramsden, 2002. Association of DNA polymerase mu (pol mu) with Ku and ligase IV: role for pol mu in end-joining double-strand break repair. *Mol. Cell. Biol*., 22 (14): 5194-5202.

47. Mari, P., Florea, B., Persengiev, S., Verkaik, N., Bruggenwirth, H., Modesti, M., . . . Van Gent, D. (2006). Dynamic assembly of end-joining complexes requires interaction between Ku70/80 and XRCC4. *PNAS,* 103(49), 18597-18602.

48. Mills, K. (2004). Rad54 and DNA Ligase IV cooperate to maintain mammalian chromatid stability. Genes & Development, 18(11), 1283-1292. doi:10.1101/gad.1204304

49. MOSHOUS, D., CALLEBAUT, I., CHASSEVAL, R., POINSIGNON, C., VILLEY, I., FISCHER, A., & VILLARTAY, J. (2003). The V(D)J Recombination/DNA Repair Factor Artemis Belongs to the Metallo-β-Lactamase Family and Constitutes a Critical Developmental Checkpoint of the Lymphoid System. Annals Of The New York Academy Of Sciences, 987(1), 150-157. doi:10.1111/j.1749-6632.2003.tb06043.

50. Murai J, Marchand C, Shahane SA, et al. (2014). Identification of novel PARP inhibitors using a cell-based TDP1 inhibitory assay in a quantitative high-throughput screening platform. *DNA Repair (Amst)* 21:177–182

51. Murai, J., Das, B., Dexhelmer, T., Takeda, S., & Pommier, Y. (2012). Tyrosyl-DNA Phosphodiesterase 1 (TDP1) Repairs DNA Damage Induced by Topoisomerases I and II and Base Alkylation in Vertebrate Cells. *The Journal of Biological Chemistry, 287*(16), 12848-12857.

52. Panier, S., & Boulton, S. (2013). Double-strand break repair: 53BP1 comes into focus. Nature Reviews Molecular Cell Biology, 15(1), 7-18. doi:10.1038/nrm3719

53. Pannicke, U., Ma, Y., Hopfner, K., Niewolik, D., Lieber, M., & Schwarz, K. (2004). Functional and biochemical dissection of the structure-specific nuclease ARTEMIS. *The EMBO Journal,23*, 1987-1997.

54. Pommier, Y., Huang, S., Gao, R., Das, B., Murai, J., & Marchand, C. (2014). Tyrosyl-DNA-phosphodiesterases (TDP1 and TDP2). *DNA Repair, 19*, 114-129.

55. Povirk, L.F. (1996). DNA damage and mutagenesis by radiomimetic DNA-cleaving agents: Bleomycin, neocarzinostatin and other enediynes. *Mutation Research, 355*, 71-89.

56. Povirk, L.F. (2013). Processing of damaged DNA ends for double-strand break repair in mammalian cells. *ISRN Molecular Biology*.

57. Povirk, L.F. and R.J. Steighner (1989). Oxidized apurinic/apyrimidinic sites formed in DNA by oxidative mutagens. *Mutation Res*. 214. 13-22.

58. Povirk, L.F., Y.H. Han and R.J. Steighner (1989). Structure of bleomycin-induced DNA double-strand breaks: predominance of blunt ends and single-base 5′ extensions. *Biochemistry*. 28, 8508-8514.

59. Povirk. L.F. and C.W. Houlgrave (1988) Effect of apurinic/apyrimidinic endonucleaser and polyamines on DNA treated with bleomycin and neocarrinostatin: specific formation and cleavage of closely opposed lesions in complementary strands. *Biochemistry*, 27. 3850-3857.

60. Povirk. L.F.. C.W. Houlgrave and Y.-H. Han, (1988). Neocarzinostatin-induced DNA base release accompanied by staggered oxidative cleavage of the complementary strand. *J. Biol.Chem.* 263. 19263- 19266.

61. Riballo, E. et al. (2004). A Pathway of Double-Strand Break Rejoining Dependent upon ATM, Artemis, and Proteins Locating to -H2AX Foci. *Molecular Cell, 16*, 715-724.

62. Rieder, S., W. Michalski, C., Friess, H., & Kleeff, >. (2011). Insulin-Like Growth Factor Signaling as a Therapeutic Target in Pancreatic Cancer. ACAMC, 11(5), 427-433. doi:10.2174/187152011795677454

63. Rosner, M., Schipany, K., & Hengstschläger, M. (2013). Merging high-quality biochemical fractionation with a refined flow cytometry approach to monitor nucleocytoplasmic protein expression throughout the unperturbed mammalian cell cycle. Nature Protocols, 8(3), 602-626. doi:10.1038/nprot.2013.011

64. Sánchez-Puig, J., & Blasco, R. (2000). Puromycin resistance (pac) gene as a selectable marker in vaccinia virus. *Gene,* 57-65.

65. Strumberg D, Pilon AA, Smith M, Hickey R, Malkas L, Pommier Y (2000) Conversion of topoisomerase I cleavage complexes on the leading strand of ribosomal DNA into 50 -phosphorylated DNA double-strand breaks by replication runoff. Mol Cell Biol 20: 3977–3987

66. Symington, L. (2002). Role of RAD52 Epistasis Group Genes in Homologous Recombination and Double-Strand Break Repair. Microbiology And Molecular Biology Reviews, 66(4), 630-670. doi:10.1128/mmbr.66.4.630-670.2002

67. Takashima, H., C. Boerkoel, J. John, G. Saifi, M.A.M. Salih, D. Armstrong, Y. Mao, F. Quiocho, B. Roa, M. Nakagawa, D. Stockton and J. Lupski, 2002. Mutation of TDP1, encoding a topoisomerase I-dependent DNA damage repair enzyme, in spinocerebellar ataxia with axonal neuropathy. Nat. Genet., 32 (2): 267-272.

68. Tsao YP, Russo A, Nyamuswa G, Silber R, Liu LF (1993) Interaction between replication forks and topoisomerase I-DNA cleavable complexes: studies in a cell-free SV40 DNA replication system. Cancer Res 53: 5908–5914

69. Umezawa, H., Maeda, K., Takeuchi, T. & Okami, Y. (1966). New antibiotics, bleomycin A and B. *J. Antibiot.* (Tokyo) 19, 200–209.

70. Van Nguyen, T., Puebla-Osorio, N., Pang, H., Dujka, M., & Zhu, C. (2007). DNA damage-induced cellular senescence is sufficient to suppress tumorigenesis: a mouse model. Journal Of Experimental Medicine, 204(6), 1453-1461. doi:10.1084/jem.20062453

71. Ward, I., Minn, K., Deursen, J., & Chen, J. (2003). P53 Binding Protein 53BP1 Is Required for DNA Damage Responses and Tumor Suppression in Mice. *Molecular and Cellular Biology,* 2556-2563.

72. Ward, J. (1990). The yield of DNA Double-strand breaks produced intracellularly by ionizing radiation: A review. *International Journal of Radiation Biology, 57*(6), 1141-1150.

73. Weterings, E., & Chen, D. (2008). The endless tale of non-homologous end-joining. Cell Res, 18(1), 114-124. doi:10.1038/cr.2008.3

74. Yang, S., Burgin, A., Huizenga, B., Robertson, C., Yao, K., & Nash, H. (1996). A eukaryotic enzyme that can disjoin dead-end covalent complexes between DNA and type I topoisomerases. *PNAS, 93*, 11534-11539.

75. Yanrong Su, J. A. (2010). Analysis of ionizing radiation-induced DNA damage and repair in three-dimensional human skin model system. *Exp Dermatol*, 16-22.

76. Zhang X, *et al* (2004) Artemis is a phosphorylation target of ATM and ATR and is involved in the G2/M DNA damage checkpoint response. Mol Cell Biol **24**: 9207–9220

77. Zhou, T. (2005). Deficiency in 3'-phosphoglycolate processing in human cells with a hereditary mutation in tyrosyl-DNA phosphodiesterase (TDP1). Nucleic Acids Research, 33(1), 289-297. doi:10.1093/nar/gki170

78. Zhou, T., Akopiants, K., Mohapatra, S., . . . Povirk, L. (2009). Tyrosyl-DNA phosphodiesterase and the repair of 3′- phosphoglycolate-terminated DNA double-strand breaks. *DNA Repair (Amst),* (8), 8-8.